

DAS Departamento de Automação e Sistemas
CTC **Centro Tecnológico**
UFSC Universidade Federal de Santa Catarina

Test-bed for feedback control of color of light of LED lamps

*Relatório submetido à Universidade Federal de Santa Catarina
como requisito para a aprovação na disciplina
DAS 5511: Projeto de Fim de Curso*

Luís Fernando Peláez Covatti

Florianópolis, Março de 2013

Test-bed for feedback control of color of light of LED lamps

Luís Fernando Peláez Covatti

Esta monografia foi julgada no contexto da disciplina
DAS5511: Projeto de Fim de Curso
e aprovada na sua forma final pelo
Curso de Engenharia de Controle e Automação

Prof. *Júlio Elias Normey Rico*

Assinatura do Orientador

Acknowledgements

I would like to acknowledge the diligent support from Dr. Robert Bunch, my supervisor at Rose-Hulman institute of Technology, who directed this project and provided me with strong background of technological and theoretical knowledge required to achieve the success we achieved.

I also thank Dr. Charles Joenathan, chair of the Department of Physics and Optical Engineering, for his support throughout the project development.

Warmest acknowledges to Dr. Julio Elias Normey Rico, my supervisor at Universidade Federal de Santa Catarina, in Brazil, for his support regarding the challenges we faced within the control design, for his help in assembling the final document and also his patience with the tight schedule.

An important factor for the success of this project that I want to acknowledge was the contribution of Ryan Chung, from Terre Haute South Vigo High School, and Eric Kercher, from Rose-Hulman, who worked with me in this project during the US summer of 2012.

This project was just possible to be developed because of the program Ciência Sem Fronteiras, sponsored by the Federal Government of Brazil and supported by CAPES (Coordenação de Aperfeiçoamento de Pessoal de Nível Superior) and IIE (Institute of International Education). I would like to extern my gratitude for being able to participate in this program and hope that this partnership between Brazil and other countries may facilitate further scientific development in our country.

The financial support from the National Science Foundation and the Smart Lighting Engineering Research under cooperative agreement EEC-0812056 is also gratefully acknowledged.

Abstract (Portuguese)

O presente projeto foi desenvolvido no Departamento de Física e Engenharia Óptica do Rose-Hulman Institute of Technology, em Terre Haute, estado de Indiana, Estados Unidos da América. O instituto é um parceiro do Smart Lighting Engineering Research Center (SLERC - Centro de Pesquisa em Iluminação Inteligente), um dos centros de excelência do National Science Foundation (NSC – Fundação Nacional de Ciência dos Estados Unidos), liderado pelo Rensselaer Polytechnic Institute (RPI), de Nova Iorque.

Motivados pelos recentes descobrimentos sobre o impacto da iluminação artificial, onipresente no cotidiano do homem moderno, na saúde humana, notadamente sobre os ritmos circadianos, buscamos desenvolver nesse projeto um sistema que seja capaz de fornecer luz com cor controlável.

O objetivo desse sistema é facilitar os estudos sendo feitos sobre os efeitos que a cor da iluminação tem sobre a saúde e o humor do ser humano. Este projeto também busca comprovar que tal objetivo pode ser alcançado com tecnologias que já possuam um custo relativamente baixo, que permita que no futuro o conceito seja aplicado a sistemas de iluminação ordinários.

Para isso, usaremos lâmpadas construídas com tecnologia baseada em LEDs (Diodos Emissores de Luz), que possui várias vantagens como maior eficiência energética e tamanho reduzido, além de ser a mais apropriada para o controle de cor.

Diferentemente do que tem sido feito em projetos semelhantes, utilizaremos controladores dinâmicos em malha fechada para garantir que a cor da luz emitida se mantenha dentro das especificações, mesmo com a presença de perturbações, como a luz solar.

Abstract

One of the many radical changes that took place in the last century was the spread of artificial lighting. This enabled society to carry out activities that were previously restricted to day time and open environments, such as social and economic, indoors and throughout night. Recent discoveries, however, have shown that the exposure to artificial light for abnormal periods may have negative impacts on health. One of the fields that have drawn the attention is how color of light plays a role on human health and mood, notably on the circadian rhythms.

This project aims to develop a system that is able to source light with controllable color and study the best ways to achieve that, using LEDs lamps, which, in addition to being suitable to such control, have many other advantages, mainly higher energy efficacy.

It was developed in the context of the Smart Lighting Engineering Research Center (SLERC), a center of excellence of the US National Science Foundation, led by Rensselaer Polytechnic Institute (RPI). It is dedicated to “The holistic integration of advanced light sources, sensors, and adaptive control architectures”. Student and faculty at Rose-Hulman are participating in smart lighting research as an outreach partner with the SLERC.

The final concept innovates by performing the light control using dynamic closed loop controller, instead of lookup tables, strategy that has been used in similar projects. It also must be composed of inexpensive technologies.

Contents

Acknowledgements.....	3
Abstract (Portuguese).....	4
Abstract	5
List of abbreviations.....	8
1. Introduction.....	9
1.1: Electric lighting.....	9
1.2: Light-Emitting Diode.....	11
1.3: Effects of lighting on humans	13
1.4: Objective	15
2. Color Science	16
2.1: What is color	16
2.2: Tristimulus values	18
3. The conceptual model	22
3.1: User Interface.....	22
3.2: Controller	23
3.3: Light Source	23
3.4: Color Detector	23
4. The Implementation	24
4.1: The LED.....	24
4.1.1: Temperature dependence	25
4.1.2: Approaching the non-linearity	25
4.2: Driver circuit	27
4.2.1: Control signals.....	27
4.2.2: Energy sourcing.....	29
4.3: Sensor.....	29
4.3.1: Use mode	30

4.4: The detector circuit.....	31
4.5: Calibration and color conversion	32
4.6: Controller	35
5. The Software	40
5.1: Interface	40
5.2: Spectrometer operation.....	45
5.3: Detectors calibration	46
5.4: Static model estimation	46
5.5: Execution of the control law	47
6. Experiments and results	49
6.1: PWM vs. Analog.....	49
6.2: Spectral data processing.....	49
6.3: Color conversion	51
6.4: Detector calibration	52
6.5: Closed loop performance	55
6.6: Costs.....	58
7. Conclusion and perspectives	60

List of abbreviations

CCT - Correlated Color Temperature

CRI - Color Rendering Index

LFL – Linear Fluorescent Lamp

HID – High-Intensity Discharge Lamp

LED – Light-Emitting Diode

PID - Proportional Integral Derivative

CIE - Commission Internationale de l'Eclairage

PWM - Pulse Width Modulated

I/O – Input/Output

IR – Infrared

UV – Ultraviolet

MIMO – Multiple Inputs / Multiple Outputs

SISO – Single Input / Single Output

1. Introduction

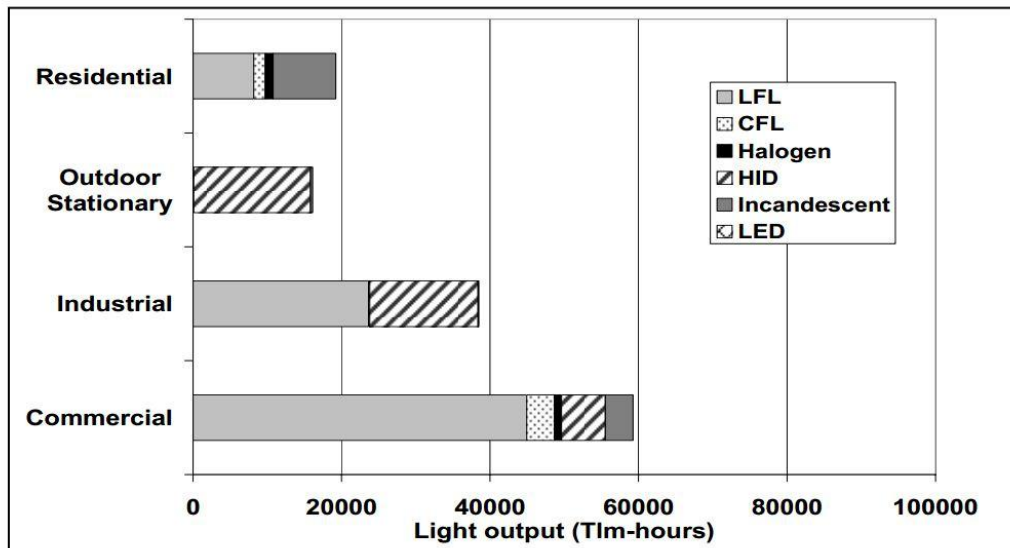
Humans are diurnal beings. We had to face many challenges that came as the sunlight faded and the night arose since the very beginning of our history. Unlike some other animals, humans' visual system is not well suitable with low levels of light. Mankind found its first way to fight against night's darkness mastering the control of fire, what happened around 400,000 years ago [1]. From this time until the XIX Century the way we produced light was always from flame produces burning some sort of combustible material, such as wood or oil.

The paradigm just started to change with the introduction of electricity. In the first decade of the XIX Century, the English scientist Humphrey Davy was the first to use electricity to generate light, using the carbon electric arc. The incandescent bulb that we are familiar with was invented several decades later by the American Thomas Alva Edison, around the 1880's.

1.1: Electric lighting

The development of electric light sources, which are cleaner, less expensive and more convenient, eventually led to their virtual omnipresence. Nevertheless, besides the numerous benefits that came with the spreading of artificial lighting, there are many drawbacks from its use that have just recently been properly taken into account. Factors such as energy efficiency and space conservation are growing concerns, since lighting accounts for approximately 20% of the end-user total electrical energy consumption in the United States [2].

The average lighting system efficacy has increased roughly three times between 1960 and 2005 [3]. However, as we see in Figure 1, by 2006 incandescent bulbs were responsible for approximately half of the artificial light produced in residential buildings around the world.



Note: LFL = Linear Fluorescent Lamps; HID = High-Intensity Discharge Lamps; LED = Light-Emitting Diodes. Source: IEA (2006).

Figure 1: Estimated light production by user sector and lamp type (2005) [3]

This means that the same technology has been used for more than a century as the main source of electrical light in residences. It is a concern since it is a very inefficient source of light, since only approximately 5% of the electrical energy is converted into light.

In fact, many technologies were developed to improve lighting efficiency and quality. In addition to efficacy (lumens/Watt), there are other aspects that are taken into account to evaluate and compare different light source technologies, such as light quality (which includes CCT and CRI), turn-on time, life-time and aging. Table 1 shows a comparison between some different lighting technologies.

Table 1: Comparison of different lighting technologies [4]

Light Source	Efficacy (lm/W)	Life (hours)*	Correlated Color Temperature (K)	Onset Time†
Tungsten filament lamp	12-20	750-4000	2700-3200	0.1-0.3 s
Fluorescent (incl. compact)	60-100	10,000-30,000	2700-7500	1-60 s
Metal halide	80-110	10,000-20,000	2800-5000	60-300 s
Xenon	30-60	1000-5000	5000-6000	1 μs
Light-emitting diode (white)	90-130	50,000-100,000	3000-8000	10-20 ns

*Assuming steady operation.

†Time to reach 90% of maximum light output.

1.2: Light-Emitting Diode

In the quest for better lighting technologies, LEDs (Light Emitting Diodes) appear as an option that combines many desired characteristics. It is a solid-state semiconductor that emits light when a current is passed through it, by electroluminescence principle [5]. *Whereas the efficiency of conventional incandescent and fluorescent lights is limited by fundamental factors that cannot be overcome, the efficiency of solid-state sources is limited only by human creativity and imagination* [6]. In fact, with today's technology, the efficacy of LED light sources can reach 10 times the efficacy of incandescent [7].

Some of the superior characteristics of the LED light sources are [8]:

- *Higher efficacy:*
- *Directional light*
- *Low profile / compact size*
- *Breakage and vibration resistance*
- *Improved performance in cold temperatures*
- *Life unaffected by rapid cycling*
- *Instant on / no warm up time*
- *No IR or UV emissions*

The so-called first wave of solid-state lighting is the attempt to develop technologies to overcome difficulties from the use of LED light sources, in order to take advantage of its benefits. The main problems that have been addressed are:

- Drop in efficiency that is observed in higher current levels
- Temperature dependence of the light emission
- The quality of light, since most cool-white LEDs have spectra that differ significantly from a black body radiator
- Higher initial costs

The progress has been so successful that the US Department of Energy has estimated that LED technology has the potential to produce yearly energy savings of 190 terawatt-hours by 2030. It is the equivalent of 24 large (1,000 MW) power plants, or the reduction of 25% of present energy consumption for lighting [9].

Nevertheless, while the first-wave has focused on changing the status-quo of lighting to LEDs, mainly because of the energy savings, the so-called second-wave of solid-state lighting, or Smart-Lighting, has approached what LED lighting systems can do to improve quality of life. The studies include applications within areas such as industry, health, communication and comfort [10].

The focus of our project is to enable the study of the impact that light has on human's health and how smart light sources can improve well-being.

1.3: Effects of lighting on humans

Many aspects of human physiology and behavior are controlled by processes that have a *circadian* rhythm, i.e., that have a cycle of approximately 24 hours. *Circadian clocks play a crucial role in the survival of organisms by appropriately scheduling their activity in the cyclic natural environment* [11]. *Examples of such processes are sleep–wake cycles, alertness and performance patterns, core body temperature rhythms, and the production of hormones such as melatonin and cortisol* [12]. In order to maintain the synchronicity with the environment, this internal clock has to be able to be reset. *The major environmental factor that resets these rhythms in humans (and mammals) is the light–dark cycle generated by the rotation of the Earth* [12]. We can see in Figure 2 an overview of the biological phenomena linked to the circadian rhythms, in their normal synchronized cycle.

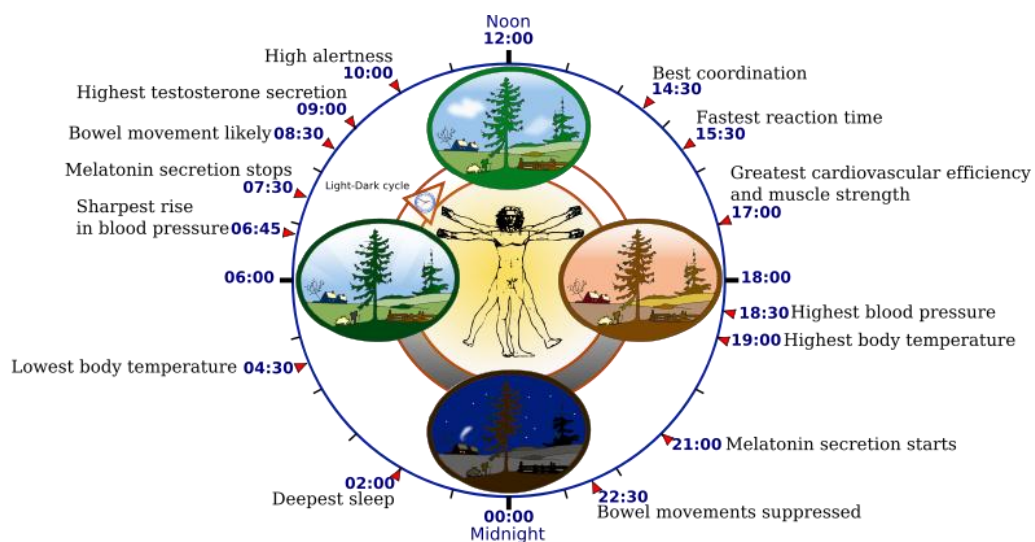


Figure 2: Overview of biological circadian clock in humans.

An evidence of how the day/night cycle affects humans is the Seasonal Affective Disorder, also known as winter blues, is the result of an over-production of melatonin, due to a lack of light. *This disorder effect occurs in regions farther from the equator, when days become shorter by fall equinox and through wintertime. A non-negligible percentage of people say they feel more depressed, have less energy, and find it difficult to wake up* [13].

In fact, *with scant exception, terrestrial organisms have evolved under predictable daily cycles owing to the Earth's rotation. The advantage conferred on*

organisms that anticipate such environmental cycles has driven the evolution of endogenous circadian rhythms that tune internal physiology to external conditions [14].

However, modern human is living under radically different lighting reality since the advent of the electrical light. Nowadays, social and economic activities are not as restricted to daytime as they were in the past. *Exposure to artificial light at night (LAN) has surged in prevalence during the past 50 years, coinciding with rising rates of depression [15].*

Because much of the daytime work force in the industrialized world is exposed to dim office lighting instead of bright sunlight, and because at night we are often exposed to bright lights with blue wavelengths instead of natural darkness, some researchers believe that adequate human circadian entrainment does not take place [16]. Dr. Mark S. Rea [17] highlights some findings about the effect of lighting on human health:

- Light can alleviate seasonal depression [18]
- Light can increase the length and quality of sleep [19]
- Light can consolidate sleep/activity patterns in Alzheimer's Disease patients [20]
- Light can improve performance of night-shift workers [21] [22]
- Light can improve weight gain in premature infants [23] [24]
- Light activation of the circadian system is affected by a newly discovered photoreceptive mechanism in the eye [25] [26]
- Light regulates melatonin [27], which has been shown to reduce breast cancer growth [28] [29]
- Light has a direct impact on cortical brain activity [30]

In addition to these extensive evidences, the discovery of a new class of cells in the retina, which are thought to be circadian rather than visual receptors, led many researchers to draw their attention to the influence of spectrum, intensity and duration of light on biological responses. However, *the range of spectra that influence the multiple circadian systems is yet to be explored [31].*

1.4: Objective

As mentioned by Eve A. Edelstein *et al* [31], the recent discoveries are leading many researchers to study the influence of color of light in human outcomes. In order to carry out such studies, it is necessary a lighting technology that allows the output of light with different colors, i.e., spectra.

Differently than any other technology, it is possible to produce LEDs that emit light with diverse dominant wave-lengths (colors), by using different semiconductor materials.

The main objective of this project is to design a system that is able to provide a large and continuous range of controlled colors of light from LED sources. It may be used in many applications where a controlled color is needed, firstly within studies on the effect of light color on health and eventually in lighting of hospitals, airplane cabins, offices, industries and homes. The cost of equipment that is needed to accomplish this goal is also a major concern to be taken into account, since the concept is to be used as common light source.

The system has also to be flexible, i.e., must allow the user to change some variables to test performance of different configurations. For instance, control strategies, LED and detector model.

As it will be explained, this controlled range of colors of light may only be achieved by a closed-loop control of multi-color LED sources. In addition, *utilizing control options of LED sources, eliminating negative aging, temperature and light color shifts, generating long-term stability and reducing potential future maintenance costs* [32].

2. Color Science

Before we proceed to the description of the project, it is important to briefly introduce some of the concepts on color of light.

2.1: What is color

Color only exists in our mind. It is a visual perceptual property that depends on the interaction of light with the human eye light receptors. The color we perceive is a result of how the spectrum of light (distribution of light power versus wavelength) excites the eye receivers. Therefore, to understand color we must take a look at the two components: the spectra of light and the eye receivers.

Light is the visible part of the electromagnetic spectrum. Light is often described as consisting of waves. Each wave is described by its wavelength. This amounts to a mere slice of the massive electromagnetic spectrum. Although we can't see them, we use many of the invisible waves beyond the visible spectrum in other ways—from short-wavelength x-rays to the broad wavelengths that are picked up by our radios and televisions.

Our eyes have light sensors that are sensitive to the visible spectrum's wavelengths. When light waves strike these sensors, the sensors send signals to the brain. Then, these signals are perceived by the brain as a particular color [...].

Passing a beam of white light through a prism disperses the light so that we can see how our eyes respond to each individual wavelength. This experiment demonstrates that different wavelengths cause us to see different colors. We can recognize the visible spectrum's dominant regions of red, orange, yellow, green, blue, indigo, and violet; and the "rainbow" of other colors blending seamlessly in between (Figure 3).

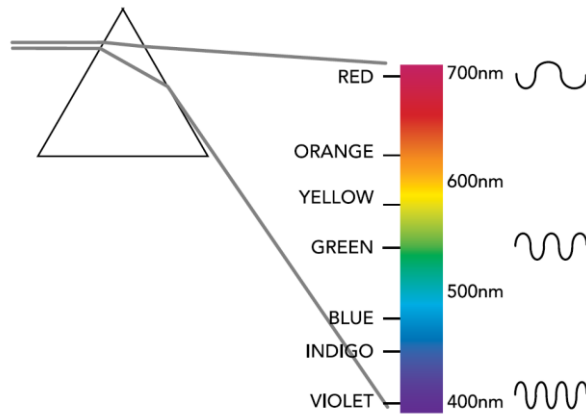


Figure 3: Light wavelengths and colors

However, we rarely see all wavelengths at once (pure white light), or just one wavelength at once. Most colors that we observe are actually a combination of light with many different wavelengths components [33].

The sensors in the eyes that are responsible for the perception of color are namely the rods and cones. The response of the rods become saturated under normal levels of luminance (photopic vision), therefore normal color perception is mediated by the response of the cones. However, the rods perform an important role at low light levels (when we see scale of gray instead of colors).

There are three types of cones, which are referred to as the short-wavelength sensitive cones (S-cone), the middle-wavelength sensitive cones (M-cones) and the long-wavelength sensitive cones (L-cones). Each one of these types has different spectral sensitivity regarding the wavelengths, as we see in Figure 4.

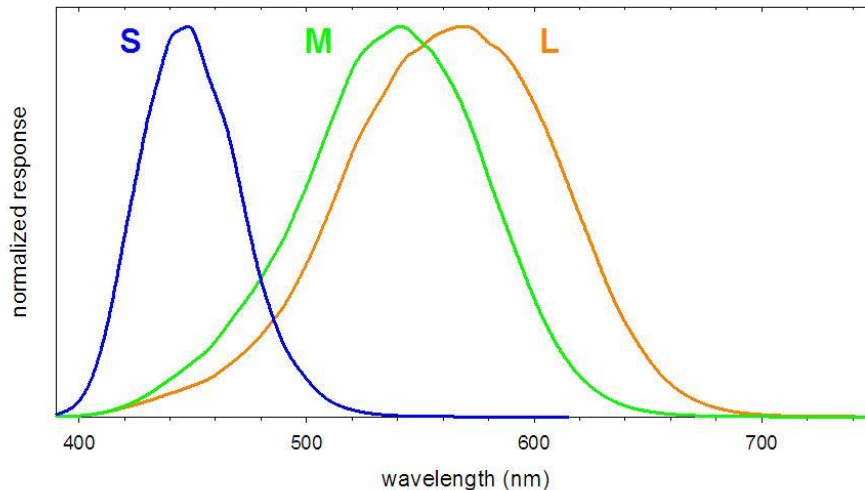


Figure 4: Spectral response of cones

Therefore, as a result of the human trichromatic nature of color vision, the same color can be perceived from many different spectra. For instance, most computer displays reproduce the spectral color orange as a combination of red and green light, instead of the pure orange wavelength. It appears orange because the red and green are mixed in the right proportions to allow the eyes' cones to respond consistently to the spectral distribution of orange. This phenomenon is called color metamerism.

2.2: Tristimulus values

The trichromatic nature of human color vision is mathematically formulated by CIE to give tristimulus values X , Y , and Z . The CIE method of colorimetric specification is based on the rules of color matching by additive color mixture. The principles of additive color mixing are known as the Grassmann's laws of color mixtures [34]:

(1) Three independent variables are necessary and sufficient for specifying a color mixture.

(2) Stimuli, evoking the same color appearance, produce identical results in additive color mixtures, regardless of their spectral compositions.

(3) If one component of a color mixture changes, the color of the mixture changes in a corresponding manner.

The basic CIE color space is CIE XYZ. It is based on the visual capabilities of a Standard Observer, a hypothetical viewer derived from the CIE’s extensive research of human vision. They used the collective results to create “color-matching functions” and a “universal color space” that represents the average human’s range of visible colors. The color matching functions are the values of each light primary—red, green, and blue—that must be present in order for the average human visual system to perceive all the colors of the visible spectrum. The coordinates X, Y, and Z were assigned to the three primaries.

The tristimulus values for a color with a spectral power distribution $I(\lambda)$ are given in terms of the standard observer by:

$$X = \int_{380}^{780} I(\lambda)\bar{x}(\lambda)d\lambda \quad Y = \int_{380}^{780} I(\lambda)\bar{y}(\lambda)d\lambda \quad Z = \int_{380}^{780} I(\lambda)\bar{z}(\lambda)d\lambda$$

Where $\bar{x}(\lambda)$, $\bar{y}(\lambda)$ and $\bar{z}(\lambda)$ are the color matching functions, specified by CIE as in Figure 5.

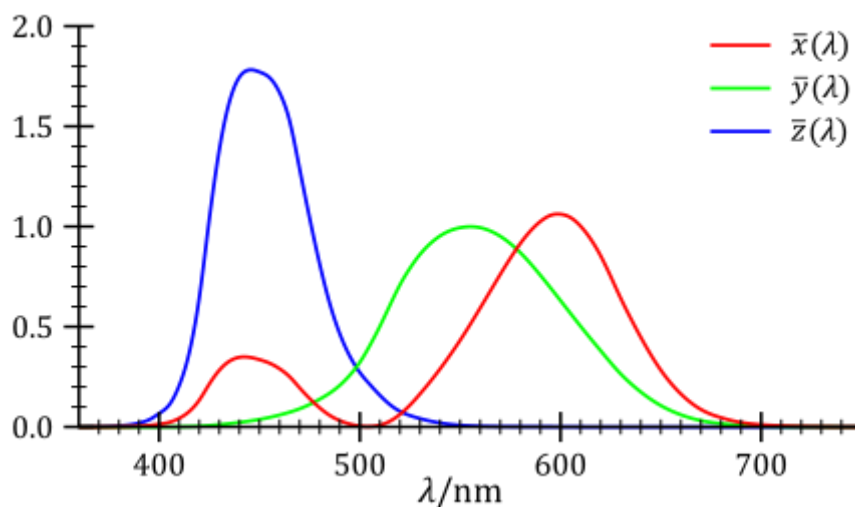


Figure 5: CIE 1931 color matching functions

Since the human eye has three types of color sensors, a full plot of all visible colors is a three-dimensional figure. However, the concept of color can be divided into two parts: brightness and chromaticity. For example, the color white is a bright color, while the color grey is considered to be a less bright version of that same white. In other words, the chromaticity of white and grey are the same while their brightness differs.

The CIE XYZ color space was deliberately designed so that the Y parameter was a measure of the brightness or luminance of a color. The chromaticity of a color was then specified by the two derived parameters x and y, two of the three normalized values which are functions of all three tristimulus values X, Y, and Z:

$$X = \frac{X}{X + Y + Z} \quad Y = \frac{Y}{X + Y + Z} \quad Z = \frac{Z}{X + Y + Z} = 1 - x - y$$

These values lead to the chromaticity diagram in *Figure 6*, which relates the values of x and y to the respective chromaticity. The outer curved boundary is the spectral (or monochromatic) locus, with wavelengths shown in nanometers. The colors are represented by brightly saturated colors. It is important to notice that different perceived colors may lead to the same point in this diagram, since it does not take into account the luminosity.

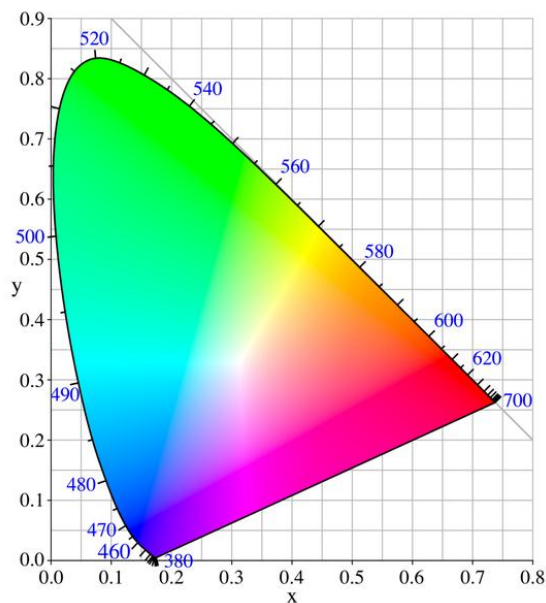


Figure 6: CIE chromaticity diagram

An important conclusion from this discussion is that any color within the visible gamut can be achieved by combining three independent components. Since light is additive, usually the three fundamental components (or primary colors) are referred to be red, green and blue. In contrast, paints and filters have subtractive behavior, which is why many mention yellow, magenta and cyan as primaries.

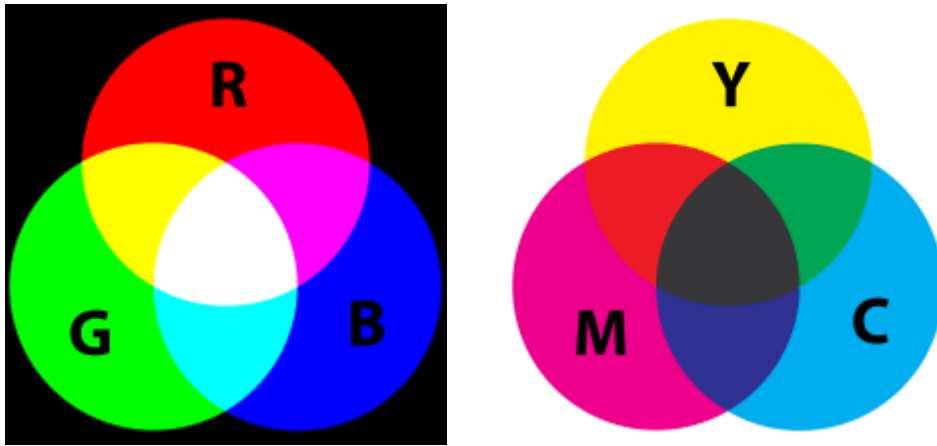


Figure 7: Additive characteristic of light (left) and subtractive characteristic of paints and filters (right)

3. The conceptual model

In order to achieve the goal of the project, which is building a system which is capable of providing light with a controlled color using LED and other inexpensive components, we must be able to:

- Provide light with different colors within a given gamut, i.e., a range of XYZ values
- Measure the color of light
- Allow the user to set the color operation point, in a given color standard
- Adjust the light color in order to achieve the desired operation point

With this in mind, the conceptual system that we want to build is described in Figure 8.

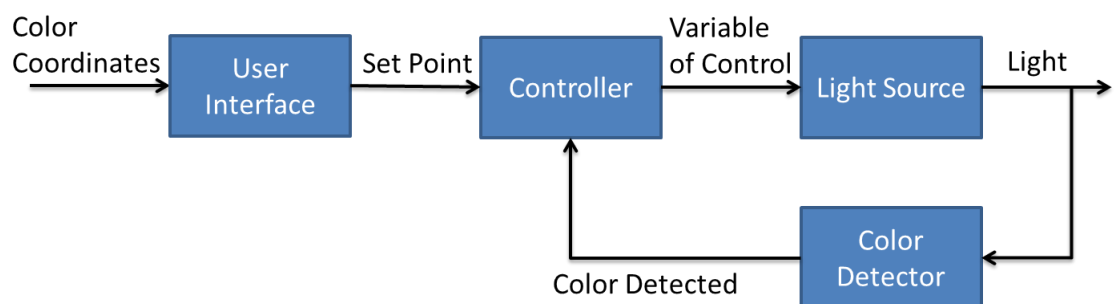


Figure 8: Conceptual model

3.1: User Interface

The system must have an interface to enable the user to set the desired color of the light. However, defining a color is not as easy as it may seem. As we saw, there are multiple ways to describe it. In fact, this must be done in a standard that the user can understand easily. CIE XYZ values will be useful in the calculations, but are not intuitive. A standard that is more intuitive is the RGB one, which has been largely used in determining color in the computational systems. It is desirable that the user interfaces is able to display the color set and being detected. It also needs to communicate with the controller subsystem, which includes translating the user commands into variables that the controller can work with.

3.2: Controller

The controller is the subsystem responsible to determine the value of the variable of control necessary at each given moment, in order to drive the system to source light with the color which was set by the user.

It will receive data from the detector and process it to determine the value of the variable of control. The nature of these variables will depend on which technology we will use, but it may be current or voltage.

It is also desirable that the user is able to define and modify the parameters of the controller, in order to test different control strategies.

3.3: Light Source

The main constrain of this project is the use of LEDs as light course, due to the advantages from it use that were described in previous chapters. This LED-based source must be able to provide light with different colors. As discussed, this can be achieved by combining at least the three primary colors of light: red, green and blue. Notice that the control on the final color will depend on how the intensity of these three components is varied. Therefore, characteristic such as linearity and wide range of operation are desirable.

3.4: Color Detector

Regarding color measurement, being able to determine the tristimulus values is sufficient to describe any color. Therefore, it is not necessary that we obtain the whole spectrum profile of the light being detected to determine its. It is important that the detectors have a fast response and linear behavior. It is also necessary that it can communicate with the controller, i.e., provide readings that are suitable to reading by the technology that will be chosen as controller.

4. The Implementation

To implement the conceptual model described in the last chapter, the following system was designed.

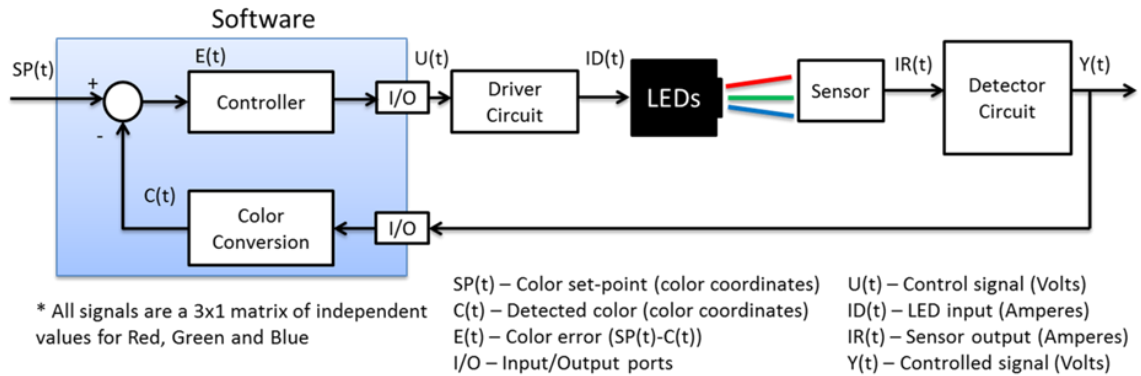


Figure 9: System model

4.1: The LED

The LED used is a high-brightness Cree® XLamp® MC-E Color LED (Figure 10). It is made out of four LEDs: one red, one green, one blue and one white.

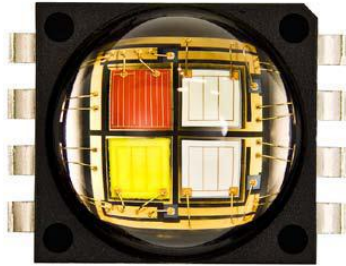


Figure 10: Cree XLamp LED

Each LED has a maximum drive current of 750 mA and a maximum power of 9.5 Watts. The spectrum of each of the LEDs can be found in the Figure 11. Different colors of light are obtained by mixing the RGB colors in different proportions. The white component may be used to achieve other lighting levels. However, the white LED will be driven to simulate disturbance.

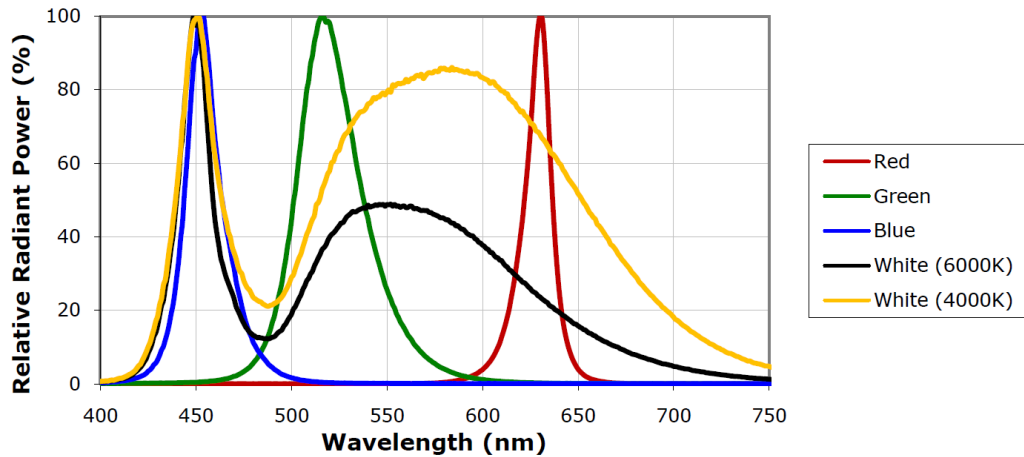


Figure 11: Spectral power distribution of the LEDs

4.1.1: Temperature dependence

LEDs have relatively high temperature sensitivity (Figure 12), i.e., the luminosity level and the spectral characteristic change depending on the temperature. It causes the color of the output light to change over time due to the heat dissipation, mainly when using high current values. In this context, closed-loop color control has the benefit of being able to readjust the LEDs current in order to bring the color back to the right value, regardless of time of usage or current level.

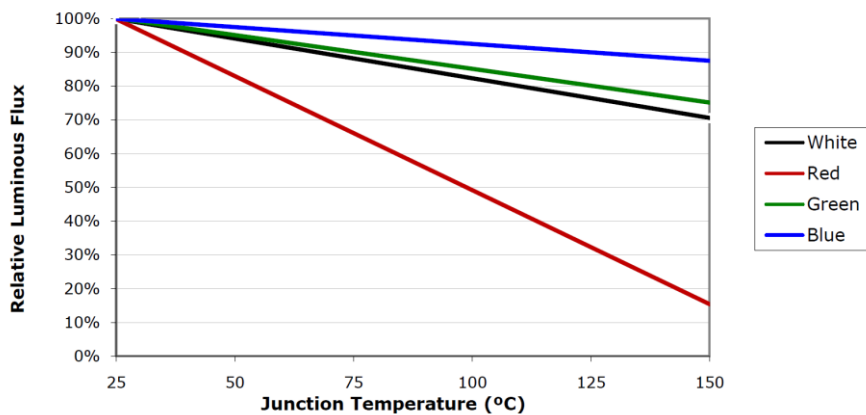


Figure 12: Temperature influence on the emission of light of the LED

4.1.2: Approaching the non-linearity

LEDs are diodes, and for this reason the relationship between the voltage and current is not linear (Figure 13), instead have a logarithmic behavior. Since the

intensity of light emitted has a *quasi-linear* relation with current (Figure 14), the relation between voltage and luminosity is also very non-linear.

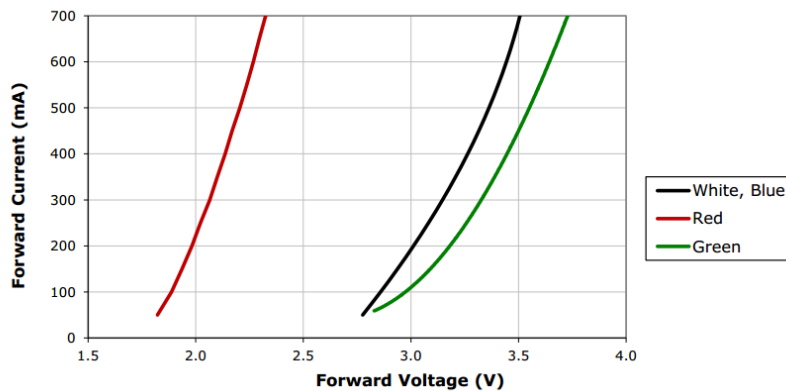


Figure 13: Electrical characteristics of each LED die (junction temperature = 25 °C)

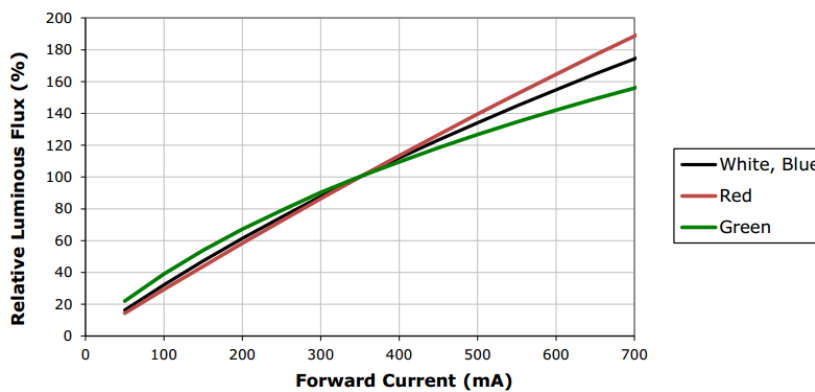


Figure 14: Relative intensity vs. current of each LED die (junction temperature = 25 °C)

As we will see ahead, the systems we have available requires us to drive the LEDs based on voltage signals. Therefore, this non-linearity would affect us directly, potentially making it very hard to control the intensity of light of each LED die and, as consequence, the color.

However, a widely used strategy to overcome this problem is the use of *pulse-width modulation (PWM)* to dim LEDs in a smooth, linear way. PWM works well with LEDs since they turn on and off in microseconds. A pulse waveform driving an LED at a frequency of several kilohertz appears to be flicker-free. Varying the pulse's duty cycle from a few percent to over 90 percent raises the LED's apparent brightness

while keeping the actual current and voltage the same [35], as it is shown in Figure 15.

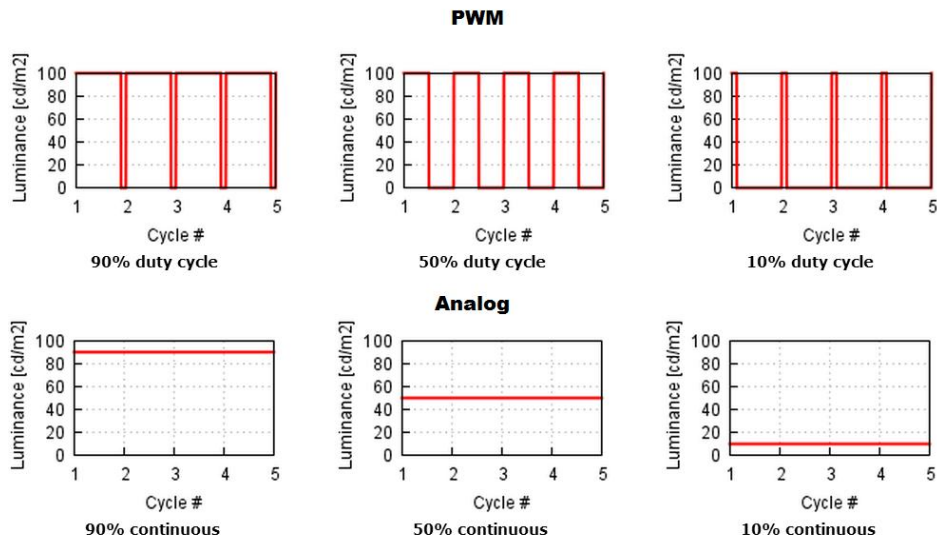


Figure 15: Comparison between PWM and analog signals

According to Simon Baker [36], besides the advantage of linearity between the driving signal (duty cycle) and intensity of light, using PWM the current can be forced to hold a constant value during the duty cycle, meaning that the characteristics that influence the color, such as temperature, remain the same, facilitating its control.

Therefore, in this project we will use PWM signals to drive the LEDs.

4.2: Driver circuit

The driver circuit is responsible to properly control the source of power to each one of the 4 LEDs, based on the signal coming from the controller.

4.2.1: Control signals

The control signals will come from an I/O board BNC 2120, manufactured by National Instruments. This board has only two PWM outputs and two analog outputs, while at least three, ideally four independent PWM signals are needed.



Figure 16: BNC 2120 I/O board

The solution we chose was to include an Arduino Leonardo as a bridge that translates the analog signals into PWM. The Arduino Leonardo has the four PWM channels that we need, with programmable resolution from 2 to 16 Bits.



Figure 17: Arduino Leonardo

Other parameter of our design is the frequency we will use for the PWM signals. It cannot be too low, which can cause that the flashing of the LEDs are perceptible; nor too high, which can cause undesirable non-linear behaviors due to the fact that the small times associated to rising and falling times become considerable when compared to the period of the PWM wave. We chose a frequency of 5 KHz, which showed to be a good compromise solution.

As we will discuss in the future work section, the Arduino may embed the controller and the interface in the future, playing the role of the computer and allowing this system to become portable and considerably less expensive.

4.2.2: Energy sourcing

Since the LEDs may consume up to 3 Watts, it is not possible to feed them directly with the controller signals, since the BNC board and the Arduino are not able to supply such a high value. Therefore, we need a separate energy source of 5 Volts and a transistor to work as an amplifier for each one of the four channels (Red, Green, Blue and White LEDs). Since we are working with PWM signals, we have the additional advantage of being able to use the transistor in its saturated mode, i.e., as a switch. It prevents the signals from any non-linearity that the inclusion of the transistor could bring. The schematic in Figure 18 shows one of the four circuits that are used to convert the lower-power PWM signals from the BNC board and the Arduino into higher-power PWM ones to feed the LEDs. Notice that the internal resistances are high enough to keep us from including a resistance in series with the LED.

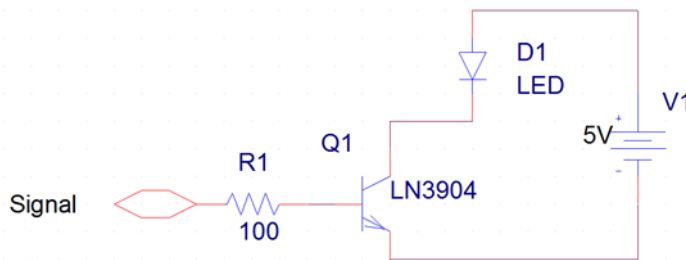


Figure 18: Sourcing-control circuit

4.3: Sensor

No control system can be better than its measurement capacity. Therefore, it is very important that the system is able to measure the controlled variables correctly in order to control them. In our case, we need to measure the color of the light with inexpensive sensors, i.e., it would not be suitable having a spectrometer, which may be very expensive, as sensor.

As it was already discussed, it is possible to determine the color of light by recognizing the intensity of red, green and blue light (relating them to XYZ coordinates). Supported by this principle, we used a RGB sensor from Hamamatsu (model S9702 - Figure 19). It consists of three photodiodes with filters in front of

them, which just let a certain range of wavelengths pass through it and reach the respective photodiode, which in turn will generate a current that is proportional to the intensity of incident light.



Figure 19: S9702 RGB Photodetector by Hamamatsu®

The response of each die of the sensor to light is shown in Figure 20. The peak sensitivity occur in the blue ($\lambda_p=460$ nm), green ($\lambda_p=540$ nm) and red ($\lambda_p=620$ nm) regions of the spectrum. The similarity of this response to the XYZ color matching functions (Figure 5) is a very important factor in measuring the color properly. In fact, this model was chosen because of its response and price.

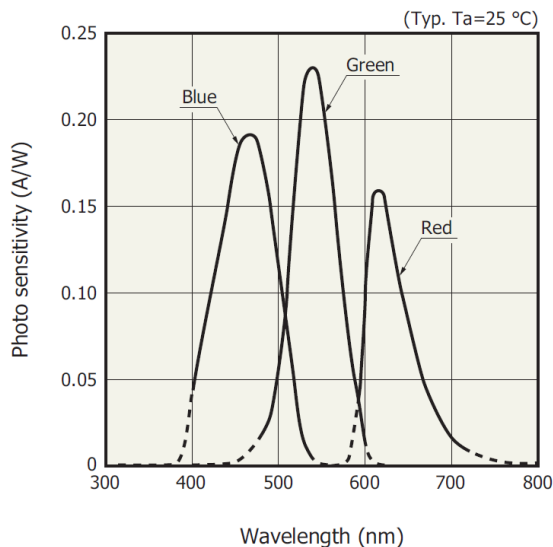


Figure 20: Spectral response of the S9702 RGB

4.3.1: Use mode

A photodiode is a *two-electrode, radiation-sensitive junction formed in a semiconductive material. [...] Each incident photon produces electron-hole pairs in the depletion region resulting in a measurable signal current. The photodiode can be operated either with zero bias in the photovoltaic mode where the photodiode is*

actually generating the electric potential supplied to the load. In a biased mode, the photoconductive mode, the reverse current is proportional to the irradiation [37].

For all practical purposes, we always use biasing because it dramatically improves the response of a photodiode [38]. The reason is that the flow of free charge carriers (what produces current) is enhanced by the external voltage (reverse bias) applied. The only drawback is the very low level of current that is provided by a diode in its reverse-bias mode. This may be overcome by connecting a high-value resistance in series, which will provide an amplified voltage signal. The value of this resistance is a trade-off between the amplification we obtain for the signal and for the noise. After testing some, we chose a value of 10 M Ω .

Therefore, in this project, we used the reverse biased mode.

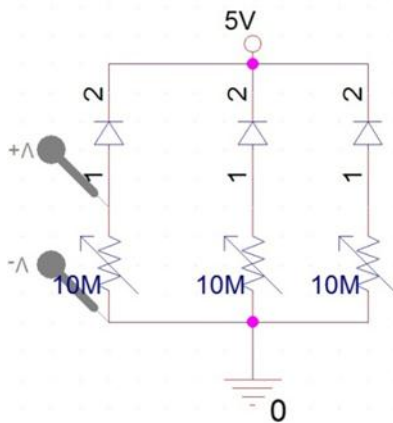


Figure 21: Reverse-biased photodiodes

4.4: The detector circuit

The current signals that are generated by the three photodiodes in the RGB sensor generate voltage signals across the series resistances. These signals have to be sent back to the computer. This communication is carried out by the BNC 2120 I/O board.

In order to avoid distortion of the signal, which may appear when the I/O board performs the sampling of the analog signal (known as aliasing); it is necessary to filter the analog signal before it is converted into digital. In addition, we have another important reason to pass the analog signal through a low-pass filter. Since we are driving the LEDs with PWM signals, even though our eyes cannot perceive the light

flashing, the photo-detectors do. To obtain a smooth curve that simulates the perception of our eyes, we need to eliminate the effect of this flashing.

Therefore, three passive low-pass filters were designed, as shown in the schematics in Figure 22. We chose passive filters since our signals will be read by a high-impedance device, so we do not need an active filter that would require additional power supply.

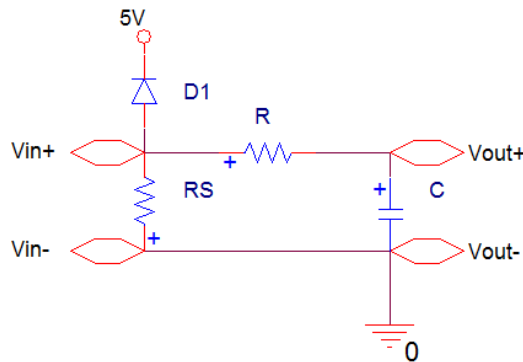


Figure 22: Detector circuit

The R and C values were determined taking into account that the cut-off frequency has to be less than 5 KHz, therefore we are using $C = 1\mu\text{F}$ and $R = 1\text{K}\Omega$, which gives a time constant $\tau=1\text{ ms}$, which is dominant when compared to the time constant of the photodiodes, which are specified to be less than $1\mu\text{s}$. Therefore, the sampling time of all readings was set to be 5 times faster, therefore 0.2 ms, or a sample frequency of 5 KHz.

4.5: Calibration and color conversion

The photodiodes will generate current, which will be passed through a circuit and be read by the I/O board as a voltage signal that is proportional to the intensity.

However, in order to determine the actual color in terms of standard coordinates, we need to calibrate the detector, i.e., find the relation between the voltages that are read and the corresponding color. In order to do that, we need an instrument that is capable of determining the color coordinates as a reference.

The instrument we used was the spectrometer Black Comet, manufactured by StellarNet®. This instrument is capable of measuring the spectral power distribution

of the incident light. As discussed earlier, it is possible to determine the XYZ color coordinates from the spectral power distribution of the light using the color matching functions.

Once having a system that determines the XYZ color coordinates, we may perform a number of experiments where we apply different colors of light and observe how the voltage of each photodiode and the coordinates read by the spectrometer evolve. Eventually, we will have two three-dimensional time series: the XYZ color coordinates (which we will call A) and the voltages of each photodiode (which we will call B). With this in hand, we want to find the relation between them, so in the future we can determine A from B , i.e., determine the XYZ color coordinates using the photodiodes instead of the expensive and slow spectrometer.

Therefore, at any instant in time i we will have:

$$A_i = \begin{pmatrix} X \\ Y \\ Z \end{pmatrix} \quad B_i = \begin{pmatrix} V_r \\ V_g \\ V_b \end{pmatrix}$$

The relation between them can be approximated by linear regressions, also known as linear least squares fittings. Multiple linear regression attempts to model the relationship between two or more explanatory variables and a response variable by fitting a linear equation to observed data. In our case, we want to find the β in the following relation that minimizes the error ε for a set of data:

$$A = \beta B + \varepsilon$$

Where:

$$\beta = \begin{pmatrix} \beta_{1-1} & \beta_{1-2} & \beta_{1-3} \\ \beta_{2-1} & \beta_{2-2} & \beta_{2-3} \\ \beta_{3-1} & \beta_{3-2} & \beta_{3-3} \end{pmatrix} \quad \text{and} \quad \varepsilon_i = \begin{pmatrix} \varepsilon_1 \\ \varepsilon_2 \\ \varepsilon_3 \end{pmatrix}$$

In such a way that at any given time i we have:

$$X_i = \beta_{1-1} V_{r-i} + \beta_{1-2} V_{g-i} + \beta_{1-3} V_{b-i} + \varepsilon_{1-i}$$

$$Y_i = \beta_{2-1} V_{r-i} + \beta_{2-2} V_{g-i} + \beta_{2-3} V_{b-i} + \varepsilon_{2-i}$$

$$Z_i = \beta_{3-1} V_{r-i} + \beta_{3-2} V_{g-i} + \beta_{3-3} V_{b-i} + \varepsilon_{3-i}$$

Notice that β is not i dependent.

Using the ordinary least squares technique, we can use the following technique to estimate β :

$$\beta \cong (B^T B)^{-1} B A$$

Once we estimate β , we can remove the spectrometer from the system and estimate \hat{X} , \hat{Y} and \hat{Z} for any instant in time i :

$$\begin{pmatrix} \hat{X} \\ \hat{Y} \\ \hat{Z} \end{pmatrix}_i = \begin{pmatrix} \beta_{1-1} & \beta_{1-2} & \beta_{1-3} \\ \beta_{2-1} & \beta_{2-2} & \beta_{2-3} \\ \beta_{3-1} & \beta_{3-2} & \beta_{3-3} \end{pmatrix} \begin{pmatrix} V_r \\ V_g \\ V_b \end{pmatrix}_i$$

However, it is important to notice that the relation β may change if some conditions change. For example, if we move the detector or the light source, the relation will change and thus the XYZ estimated. Therefore, it is important that this process is possible to be done automatically, once having the spectrometer connected. Both automatic calibration and color interpretation are done by the software we developed.

It is important to mention that most computational components work with a different standard than the XYZ coordinates, which is not very intuitive. The most widely used is the RGB system, which specifies values for Red, Green and Blue in a scale of integer numbers from 0 to 255, providing more than 15 million possible color combinations [39]. There are many RGB color space, and we will use the color space, which was proposed by Hewlett-Packard and Microsoft.

This sRGB coordinates (R G B) can be approximated from the XYZ coordinates the following conversion [40]:

$$\begin{pmatrix} R_{lin} \\ G_{lin} \\ B_{lin} \end{pmatrix} = \begin{pmatrix} 3.2404542 & -1.5371385 & -0.49853148 \\ -0.9692660 & 1.8760108 & 0.0415560 \\ 0.0556434 & -0.2040259 & 1.0572252 \end{pmatrix} \begin{pmatrix} X \\ Y \\ Z \end{pmatrix}$$

$$R = 255 \times (R_{lin})^{\frac{1}{2.2}}$$

$$G = 255 \times (G_{lin})^{\frac{1}{2.2}}$$

$$B = 255 \times (B_{lin})^{\frac{1}{2.2}}$$

The standard sRGB system produces colors that are within the following region of the chromaticity diagram (*Figure 23*), or gamut:

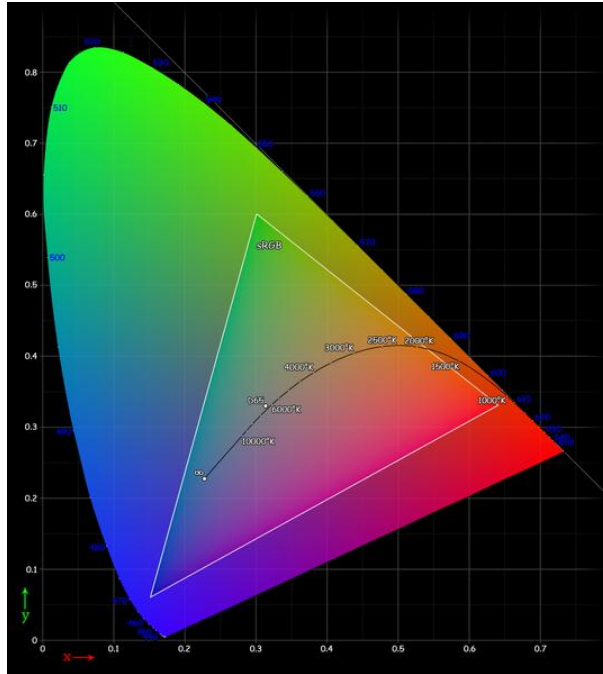


Figure 23: sRGB color gamut

4.6: Controller

The controller subsystem is the responsible for calculating what currents have to be supplied to each one of the three LEDs in order to match the color coordinates that are read by the detector subsystem to the ones input by the user.

The controller used as base is a PI, i.e., a PID without the derivative action, whose equation follows bellow:

$$MV(t) = K_p \left(e(t) + \frac{1}{T_i} \int_0^t e(\tau) d\tau + T_d \frac{d}{dt} e(t) \right)$$

Where $MV(t)$ is the control action (or the Manipulated Variable), $e(t)$ is the error, K_p is the proportional gain, T_i is the integral time, and T_d is the derivative time (set to zero in a PI).

The proportional term produces an output value that is proportional to the current error value (related to present error). The integral in a PID controller is

proportional to the sum of the instantaneous error over time (related to past error). The derivative action is calculated by determining the slope of the error (related to a prediction of the future error).

In addition, it is important to highlight that null steady-state error is only possible when integral action is included and that including derivative action might amplify the noise.

Since rise time is not a major issue in our system, due to its original fast response times, we decided to use a PI with conservative gains. This creates minimal overshoot, eliminates the steady-state error, and does not amplify the noise. The resulting block diagram is shown in Figure 24, where PV is the process variable, SP is the set-point and K_i is the ratio K_p/T_i .

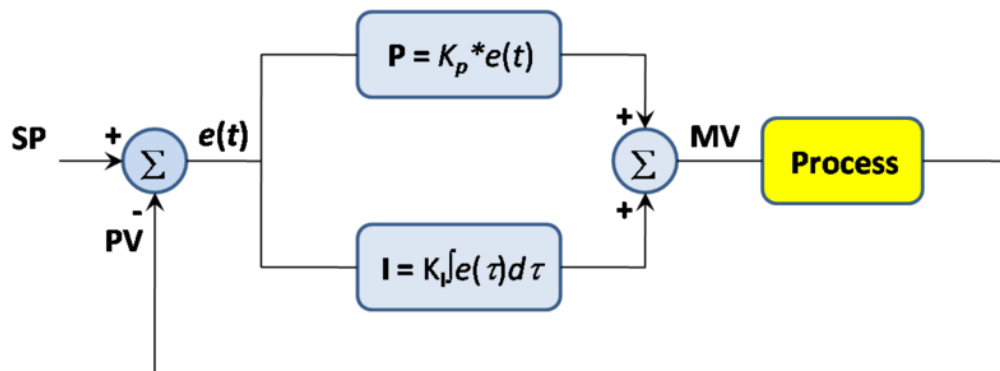


Figure 24: Generic PI block diagram

The transfer function $C(s)$ that relates the error $e(s)$ and the manipulated variable $MV(s)$ is given by:

$$\frac{MV(s)}{e(s)} = C(s) = K_p \frac{(1 + sT_i)}{sT_i}$$

However, we cannot forget that we are dealing with a multiple-input multiple-output system: we have three manipulated variables, i.e., outputs (duty cycle of the red, green and blue LEDs) and three control variables, i.e., inputs (\hat{X} , \hat{Y} and \hat{Z}). We could try to deal with them as three independent single-input single-output systems. However, the performance of such approach is subject to how independent the systems actually are, i.e., how coupled they are.

In fact, after testing the independence of the variables, we obtained the following map of gains, i.e., how each manipulated variable affect each process

variable. It was obtained by changing the intensity of one LED at a time and observing how each of the photodiodes responds in steady state.

Table 2: Map of static gains Input/Output

R_read		2.5914	0.1127	0.0138		R_out
G_read	=	0.003	0.2729	0.0289	*	G_out
B_read		0.0697	0.2509	4.1283		B_out

The correlation between them is observed to reach up to 10%, which indicates that an actual SISO control design could perform better. This behavior may be explained by the difference between the spectral distribution of each LED die and each one of the filters spectral response.

Therefore, we implemented a PI controller that takes into account the cross-relation between the input and output variables. It is done by applying the same PI on the signals and then merging them with a weighting matrix that tries to lighten the correlation effects, or decouple the variables. This effect is achieved by the following control law. Let R_{out} , G_{out} and B_{out} be the output signal to the red, green and blue LED dies respectively, in duty cycle; X_{sp} , Y_{sp} and Z_{sp} be the CIE XYZ coordinates obtained from the RGB set-point values specified by the user; \hat{X} , \hat{Y} and \hat{Z} be the XYZ coordinates estimated from the photodiodes readings; and P_{est} the estimated static model.

$$\begin{pmatrix} R_{out} \\ G_{out} \\ B_{out} \end{pmatrix} = P_{est}^{-1} \times C(s) \times \begin{pmatrix} X_{sp} - \hat{X} \\ Y_{sp} - \hat{Y} \\ Z_{sp} - \hat{Z} \end{pmatrix}$$

However, notice that the output signals are duty cycles hence limited to vary within 0 and 1. The saturation of the manipulated variables may cause an effect known as integrator windup.

When a set-point change is applied, the control variable might attain the actuator limit during the transient response. In this case the system operates as in the open-loop case, since the actuator is at its maximum (or minimum) limit, independently of the process output value. The control error decreases more slowly as in the ideal case (where there is no saturation limits) and therefore the integral term becomes large (it winds up). Thus, even when the value of the process variable

attains that of the reference signal, the controller still saturates due to the integral term and this generally leads to large overshoots and settling times [41]. Another situation that will be common in our application is that the set-point color coordinates are out of the gamut that can be achieved by the LEDs. In this case, the LED will saturate (either completely turned on or off), thus the error will not decrease and the integrative component will become larger indefinitely. When the set-point is brought back within the range, the integrative term will still be so large that it may take a considerable amount of time before the system compensate it and reaches the desired value.

To overcome this problem, we used the so-called Back-Calculation and Tracking strategy, which work as follows: when the output saturates, the integral term in the controller is recomputed so that its new value gives an output at the saturation limit. The block diagram of a generic PI with this anti-windup strategy is shown in Figure 25.

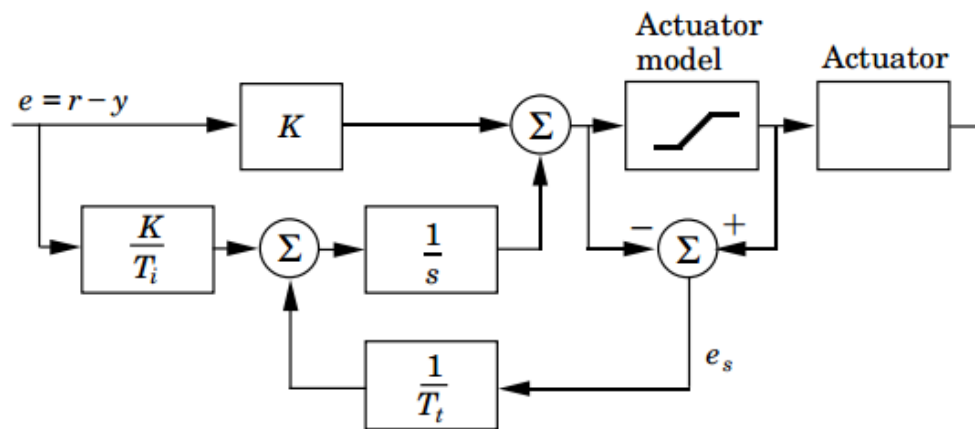


Figure 25: Generic PI controller with anti-windup

The system has an extra feedback path that is generated by measuring the actual actuator output and forming an error signal (e_s) as the difference between the output of the controller (v) and the actuator output (u). Signal e_s is fed to the input of the integrator through gain $1/T_t$. The signal is zero when there is no saturation. Thus, it will not have any effect on the normal operation when the actuator does not saturate. When the actuator saturates, the signal e_s is different from zero.

The rate at which the controller output is reset is governed by the feedback gain, $1/T_t$, where T_t can be interpreted as the time constant, which determines how quickly the integral is reset. We call this the tracking time constant [42].

Small values [...] chosen for T_t decrease the saturation time of the controller output and also the settling time of the process. In that case, the process response will be slow and will not produce an overshoot. Big values [...] chosen for T_t provide a long saturation time at the controller output and it will also produce over-shoots in the system response; that is, the system response will be fast but with an over-shoot [43].

We will address the implementation of the controller in Figure 25 when we analyze the software, which will emulate a discrete version of it.

We can see that the map of gain is a component of the control law. Since the map is also susceptible to change, it would also be important to perform automatically the experiment that maps the correlation between inputs and outputs. This feature is also performed by the software.

Finally, it is important to mention that the parameters K_p and K_i must be possible to be set by the user.

5. The Software

Complex software had to be developed to serve as the interface through the user will input color set points and parameters, such as the controller ones, and observe the status of system variables, such as color being detected. In addition, at this point we identified many other features that it must include, such as:

- Operation of the spectrometer and color conversions
- Automatic calibration of the detectors
- Automatic estimation of static model
- Execute the control law

To achieve these and other features, we developed the software in LabView®.

5.1: Interface

To better explain the functioning of our software program, we start by analyzing the front panel of it, which is shown in Figure 26:

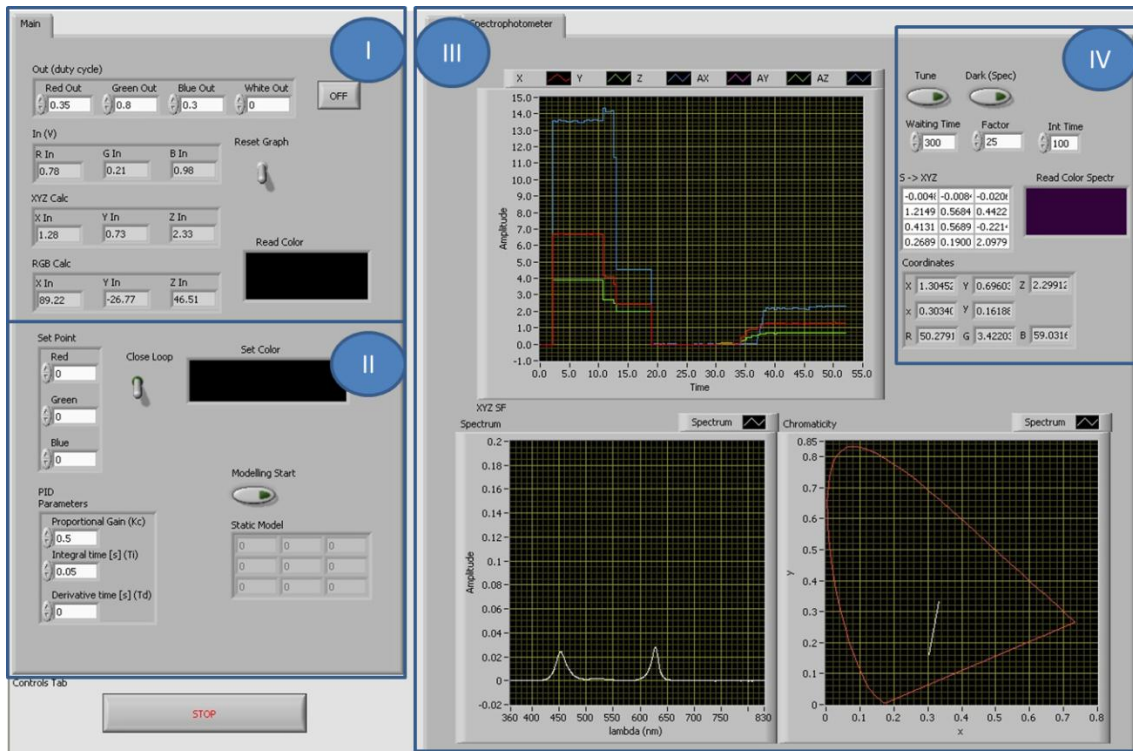


Figure 26: Software front panel

The group I encompasses the following components:

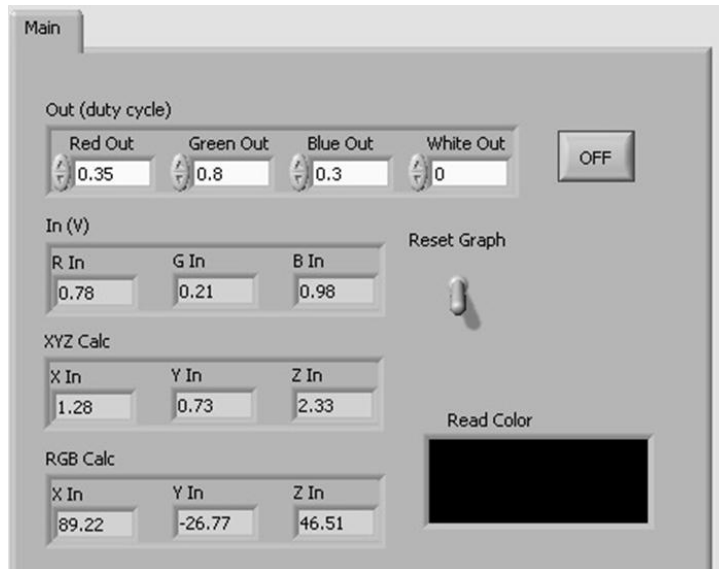


Figure 27: Software front panel components, group I

- Out (duty cycle): Control cluster that contains the fields where the output signal to each LED is specified, either by the program or by any other part of the software. It is given in terms of Duty Cycle, from 0 to 1.
- In (V): Indicator cluster which displays the raw values that are being read from the BNC board, before any conversion, thus in Volts.
- XYZ Calc: Indicator cluster that displays the XYZ coordinates being read, which is obtained from the voltages.
- RGB Calc: Indicator cluster that displays the RGB coordinates obtained from the calculated XYZ values using approximate sRGB color space.
- Read Color: Color box indicator to display on the screen the color being detected, based on the RGB Calc values
- Reset graph: Button to reset the coordinates time-series graph
- OFF: Button to set all LED outputs to 0.

The group II encompasses the following components:

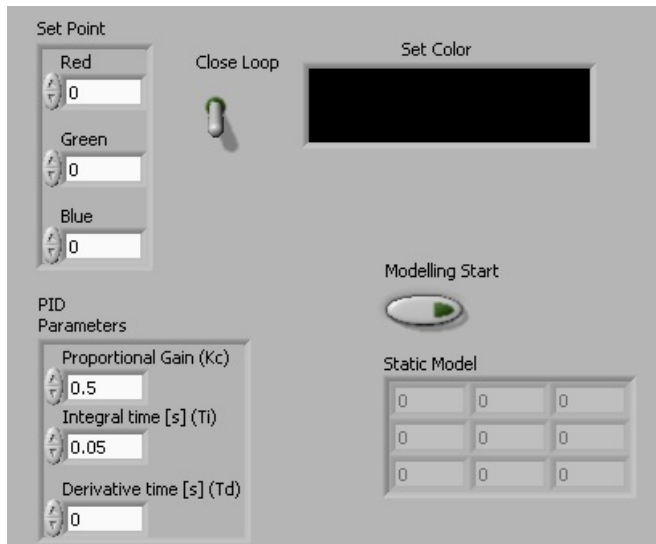


Figure 28: Software front panel components, group II

- Set Point: Cluster control where the color set point is input. It must be done in RGB coordinates.
- Set Color: Component that displays the color set. It also may be used to select the color using the interface in Figure 29.

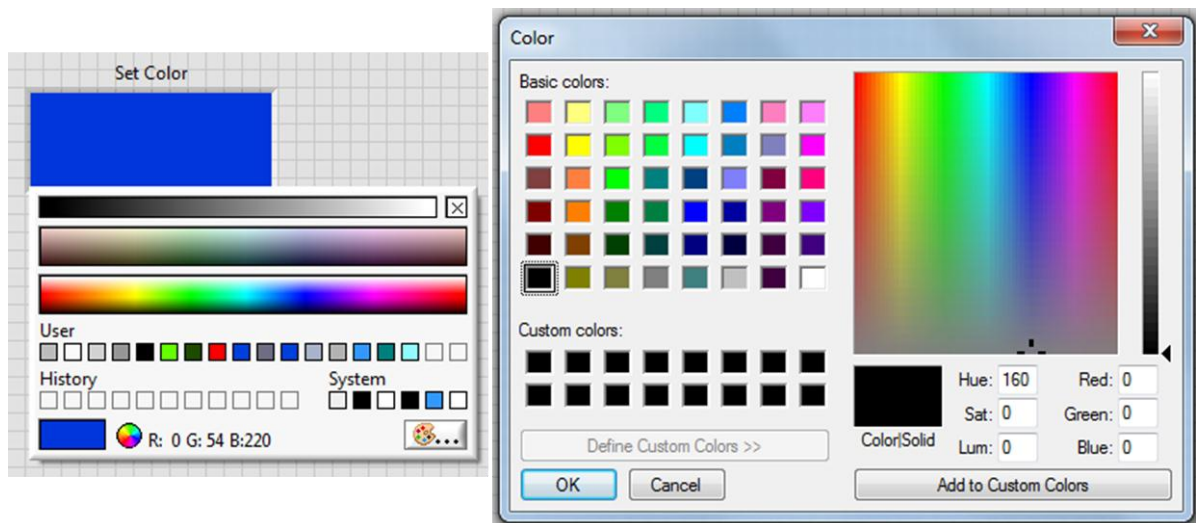


Figure 29: Interface to set color

- Close Loop: Switch to turn on and off the closed loop control of the color.
- PID Parameters: Cluster control where the controller parameters (proportional gain K_c , integral time T_i and derivative time T_d) can be specified. Changing T_d does not have impact, since we use a PI.

- Modeling Start: Button to trigger the automatic calculation of the static model.
- Static Model: Indicator matrix that contains the static model that was calculated and is being used.

The group III includes the following components:

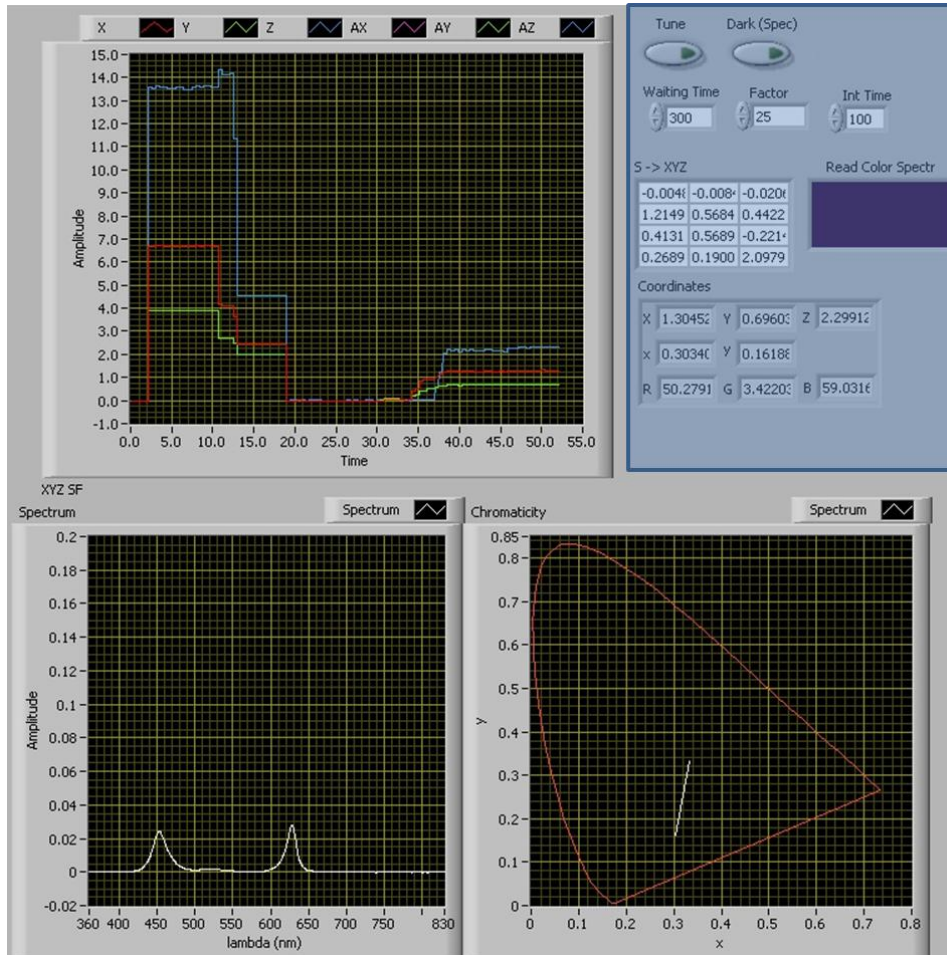


Figure 30: Software front panel components, group III

- XYZ SP: Chart that displays the time series values of the $\hat{X}\hat{Y}\hat{Z}$ coordinates that are estimated from the detectors' readings and the XYZ coordinates read by the spectrometer.
- Spectrum: Chart that displays the spectral power distribution of the light being detected, provided by the spectrometer (when it is connected).
- Chromaticity: Chart that displays the CIE chromaticity diagram, specifying the chromaticity point of the detected color, given by the xy values provided by the spectrometer.

The group IV includes the following components:

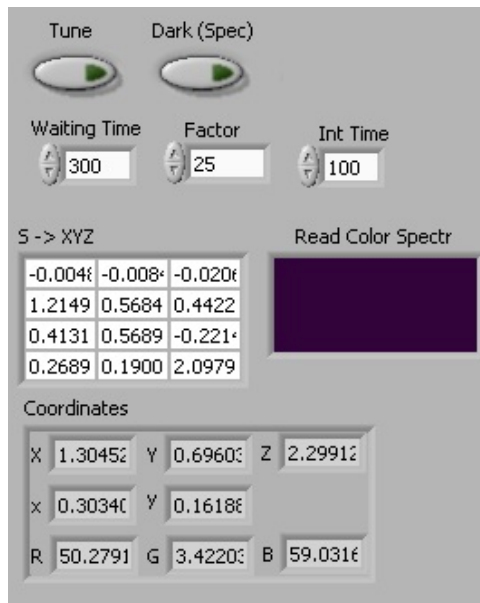


Figure 31: Software front panel components, group IV

- **Tune**: Button that triggers the automatic calibration of the photodiodes.
- **Dark (Spec)**: Button that captures the spectrum that will be used as dark reference when pressed, from that point on.
- **Waiting time**: Control that specifies the time between two consecutive the steps of the automatic calibration.
- **Factor**: Control that specifies the scaling factor for the calculation of the XYZ coordinates from the spectrum provided by the spectrometer.
- **Int Time**: Define the integration time of the spectrometer.
- **S->XYZ**: Matrix containing the calibration values for the transformation between XYZ and $\hat{X}\hat{Y}\hat{Z}$.
- **Read Color Spectr**: Color box that displays the color being read by the spectrometer.
- **Coordinates**: Indicator cluster containing the XYZ coordinates obtained from the spectrometer and the associated chromaticity xy and RGB coordinates, which are obtained from the XYZ values.

Notice that the groups III and IV are just active when the spectrometer is connected, with the exception of the XYZ SP, which displays the estimated values $\hat{X}\hat{Y}\hat{Z}$ even when the spectrometer is not connected.

5.2: Spectrometer operation

As we saw in the last section, much information is to be obtained from the spectrometer. The final goal of this data is allowing the calibration of our detector system. The manufacturer StellarNet® provides a software with the spectrometer, called SpectraWiz®, which is capable of performing a wide set of analysis on the spectral distribution detected by the device. This data comprises many color coordinates systems, including the CIE XYZ color space that we are interested in.

We need this data to be obtained on-line in the LabView program. StellarNet provides a toolkit to be used in LabView environment. However, the toolkit just provides the raw spectral power distribution, i.e., a sequence of values related to power, one for each wavelength, at a given instant in time. It means that we need to determine the XYZ color coordinates from this spectral distribution *by hand*.

However, this raw data is given in terms of *counts per sample* for each wavelength. In order to apply the color matching functions, we need to have the spectrum in terms of *Watts* per each wavelength. Fortunately, StellarNet provides a calibration file, which can be used to convert the power distribution from counts/sample into *Watts*.

The mathematical process of obtaining XYZ values using the CIE color matching functions was discussed in 2.2:Tristimulus values. But before performing this calculation, we need to take a dark reference, which is the equivalent of zeroing the instrument. That is to be done manually by pressing the Dark (Spec) button when the spectrometer is in a dark environment. It will save the spectrum read at that instant and subtract it from all the spectra read from this time on.

Another important parameter that has to be defined is the integration time of the spectrometer. This is the amount of time (in milliseconds) that the spectrometer records for a single measurement, which can influence the correct measurement. Small integration time leads to loss of sensitivity, while large values may cause the detector to saturate. The factor that is specified in the front panel may be used to compensate the influence of the integration time.

The spectral distribution resultant from the difference between the raw data and the dark reference and converted into *Watts* is displayed in the chart *Spectrum*.

The XYZ values obtained from the spectral distribution are the ones displayed in the *Coordinates* cluster, as well as the *xy* and RGB calculated from these values. In turn, the color box *Read Color Spectr* uses the RGB values to display the respective color.

5.3: Detectors calibration

An important task that the software carries out is the automatic calibration of the detectors, by using the reference data from the spectrometer. The mathematical process involved with it was discussed in section *4.5: Calibration and color conversion*.

To find the matrix β we need two time series, one containing n values of XYZ read by the spectrometer, and other containing n values of (V_r , V_g and, V_b), i.e., the voltages read from the photodiodes.

The automatic calibration process starts when the user turns the button *Tune* on. From this time, the system will scan the voltages and the XYZ values and append them to a respective array. In order to have a more robust calibration, it is desirable that we do it using data from different operation points. Therefore, at every amount of time specified by the *Waiting Time* control in the front panel, a new operation point is randomly set, i.e., we randomly change the values of the *Out (duty cycle)* control. In order to not let the transient state influence the calibration, the recording of the variables is briefly paused after a change of operation point.

This tracking will keep going until the user turns the *Tune* button off. At the end of this process, we will have the two arrays we need to perform the least square fitting and find the matrix β that will be used to estimate $\hat{X}\hat{Y}\hat{Z}$ from that point on. The more data it is obtained, the better the calibration tends to be.

5.4: Static model estimation

As discussed in the section *4.6: Controller*, we need to estimate the static model of the system in order to be able to apply a MIMO control strategy. This estimation starts when the user activates the button *Modeling Start* on the front panel. The software is programmed to apply a sequence of steps in the output value of every LED, one at a time. During this time, the system keeps track of the output

variables, as well as of the $\hat{X}\hat{Y}\hat{Z}$ coordinates. The recording makes a small pause after the application of every step, to keep the transient dynamics from influencing the static model. At the end of the routine, we will have two arrays containing the time series of these values. The static model is then found in the same way we found the relation in the calibration, i.e., by using least squares.

5.5: Execution of the control law

The software is also responsible for performing the calculations needed to apply the PI anti-windup controller we discussed in 4.6: *Controller*.

The calculations to determine the manipulated variables will be done once every cycle. It means that we have to replace the continuous models we had by discrete versions of them.

The control law applied by the software is given by:

$$\hat{R}_{out}[n] = Kp \cdot \left(e_r[n] - e_r[n-1] + \frac{T_s}{T_i} e_r[n] \right) + Sat_r[n] \cdot \frac{T_s}{T_t} + \hat{R}_{out}[n-1]$$

Where:

$$e_r[n] = X_{sp}[n] - \hat{X}[n]$$

$$Sat_r[n] = \begin{cases} 1 - R_{out}[n-1], & R_{out}[n-1] > 1 \\ -R_{out}[n-1], & R_{out}[n-1] < 0 \\ 0, & \text{Otherwise} \end{cases}$$

The $\hat{G}_{out}[n]$ and $\hat{B}_{out}[n]$ are obtained by the same method. The final control variable is given by:

$$\begin{pmatrix} R_{out} \\ G_{out} \\ B_{out} \end{pmatrix} = P_{est}^{-1} \cdot \begin{pmatrix} \hat{R}_{out} \\ \hat{G}_{out} \\ \hat{B}_{out} \end{pmatrix}$$

Where T_s is the sample time (0.2 ms in our case). The block diagram of the complete controller is shown in Figure 32.

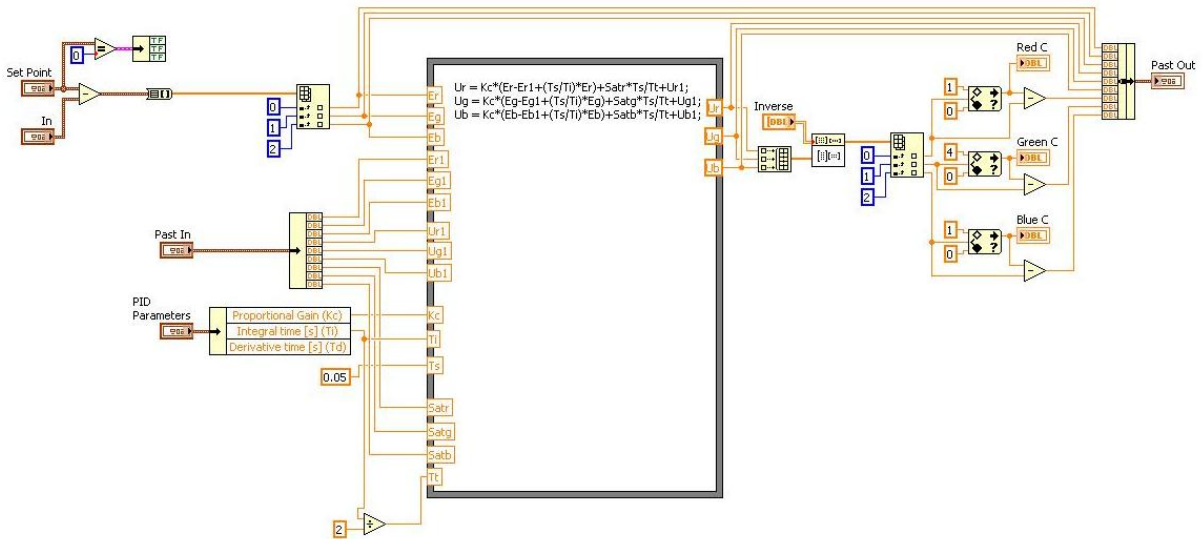


Figure 32: Controller implementation in LabView

6. Experiments and results

In this chapter, we will first analyze some of the results we obtained from using the approaches we chose to address some of the problems that appeared. Finally, we will analyze how the system fulfills the overall requirements.

6.1: PWM vs. Analog

In the Figure 33 we can observe that the PWM driving strategy produces a very linear response for luminosity versus duty cycle. In the other hand, the response to analog voltage signals has a very non-linear behavior, including a dead-zone, due to the fact that a diode must be polarized with a minimum before it can conduct. Since the diode that is subject to PWM signals is always under 0 or 5 Volts, this dead-zone does not appear. In fact, the coefficient of determination R^2 obtained with the PWM response is 0.9997, against 0.8382 of the analog response.

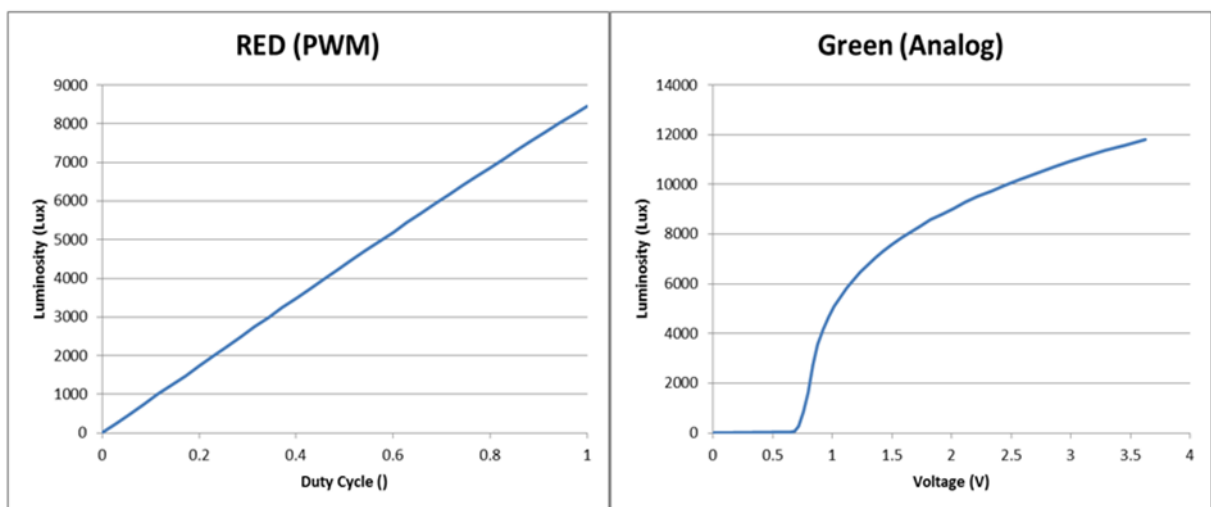


Figure 33: PWM vs. Analog

6.2: Spectral data processing

As we discussed in 5.2: *Spectrometer operation*, our software has to process the data from the spectrometer in order to extract useful information, namely the XYZ color coordinates. The first challenge was to convert the units of the raw data. The

relation between counts/sample and Watts/m² is not just a constant scaling factor, it is necessary rather to apply specific calibration factor to each wavelength. The calibration curve is shown in Figure 34.

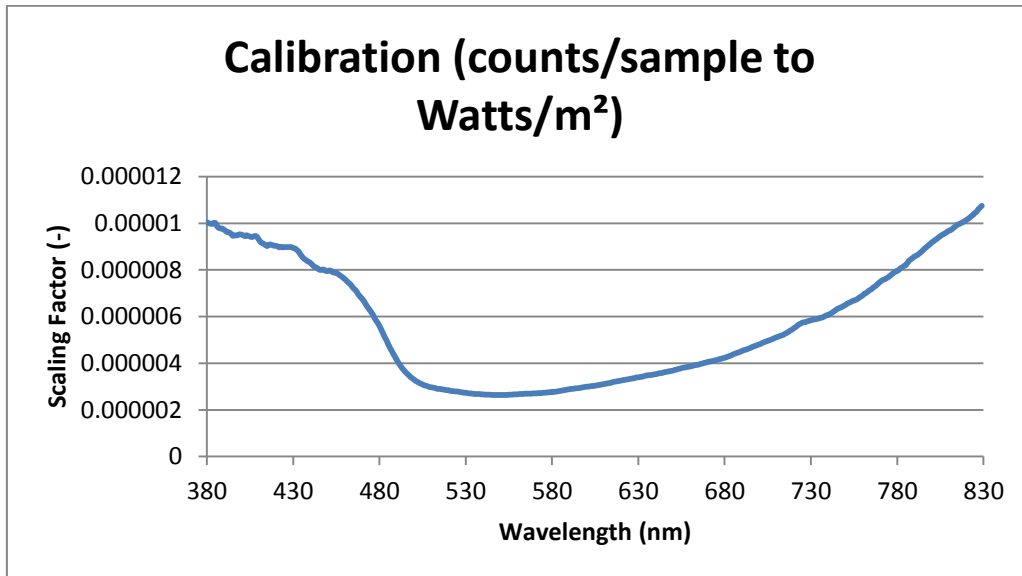


Figure 34: Calibration curve

In fact, after multiplying the raw data we have by the calibration curve we expect to have a result that is very similar to the readings in Watts performed by the SpectraWiz software. In fact, we obtain the results in Figure 35.

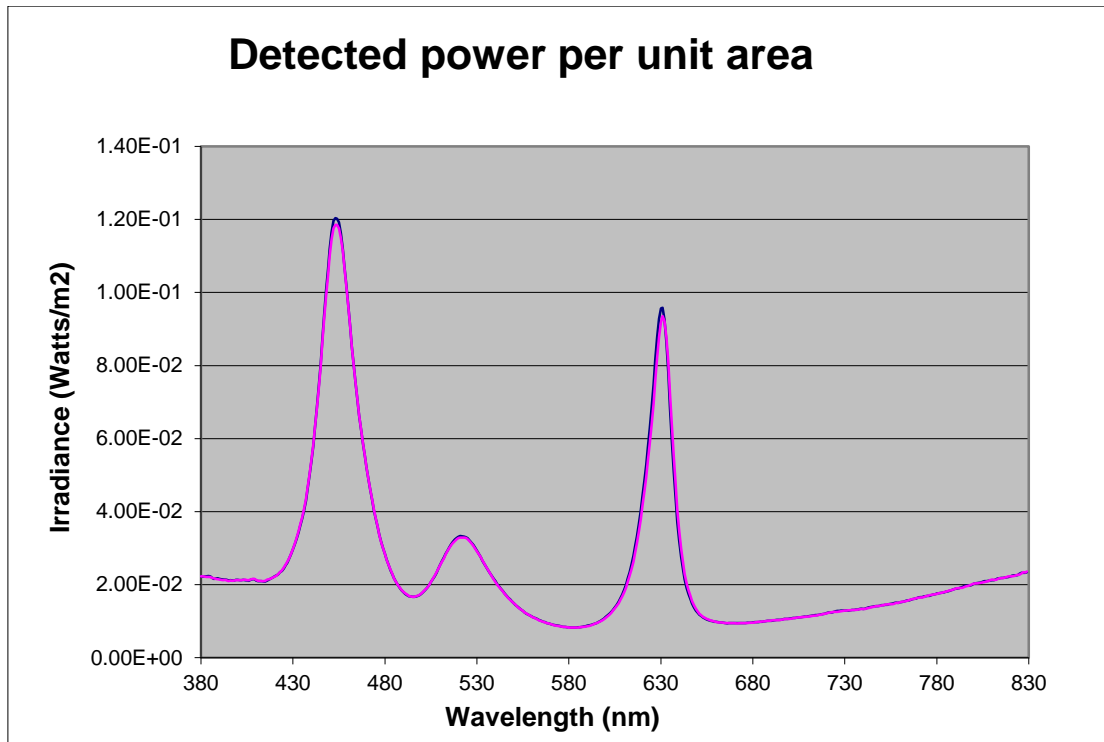


Figure 35: Comparison between calculated and given irradiance in Watts/m²

The average error obtained is 1.49%, which is a very good approximation, since errors of the same magnitude (up to 2%) may be obtained between two consecutive readings of the spectrometer.

6.3: Color conversion

Once with the spectral power distribution in hand, we must assure that we can determine the right color. We need to obtain RGB values that generate colors similar to those being detected. Since the SpectraWiz software does not provide us with this sort of coordinates, the way to empirically evaluate the performance is by comparing the colors displayed by the color boxes of our front panel to a picture.

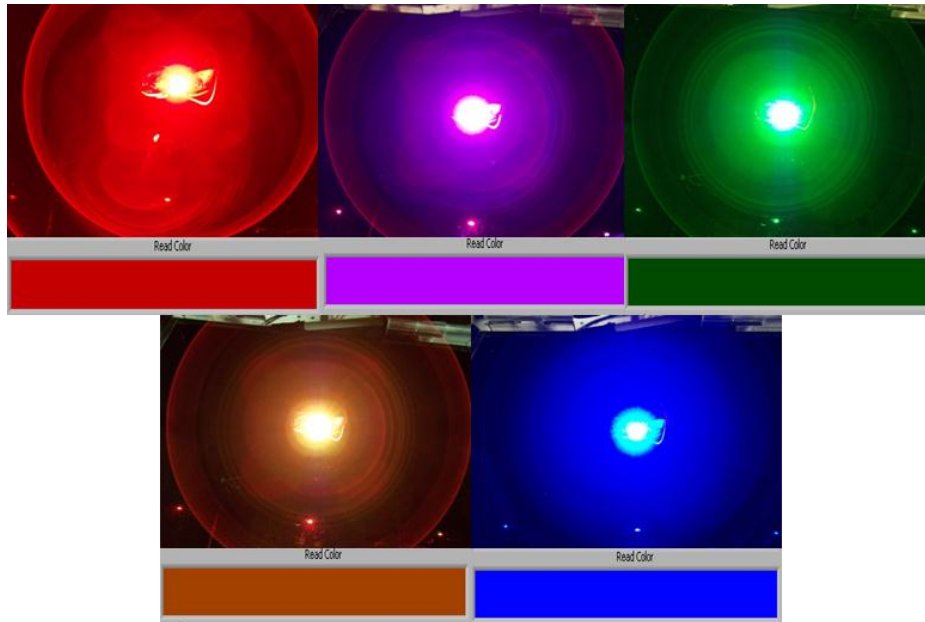


Figure 36: Comparison between the detected and calculated color

6.4: Detector calibration

Besides calculating properly the color coordinates from the spectral power distribution, it is necessary that we can properly relate the readings from the photodiodes to those of the spectrometer.

If we just use the red, green and blue LEDs both to calibrate and to test the calibration, we obtain the result in Figure 37.

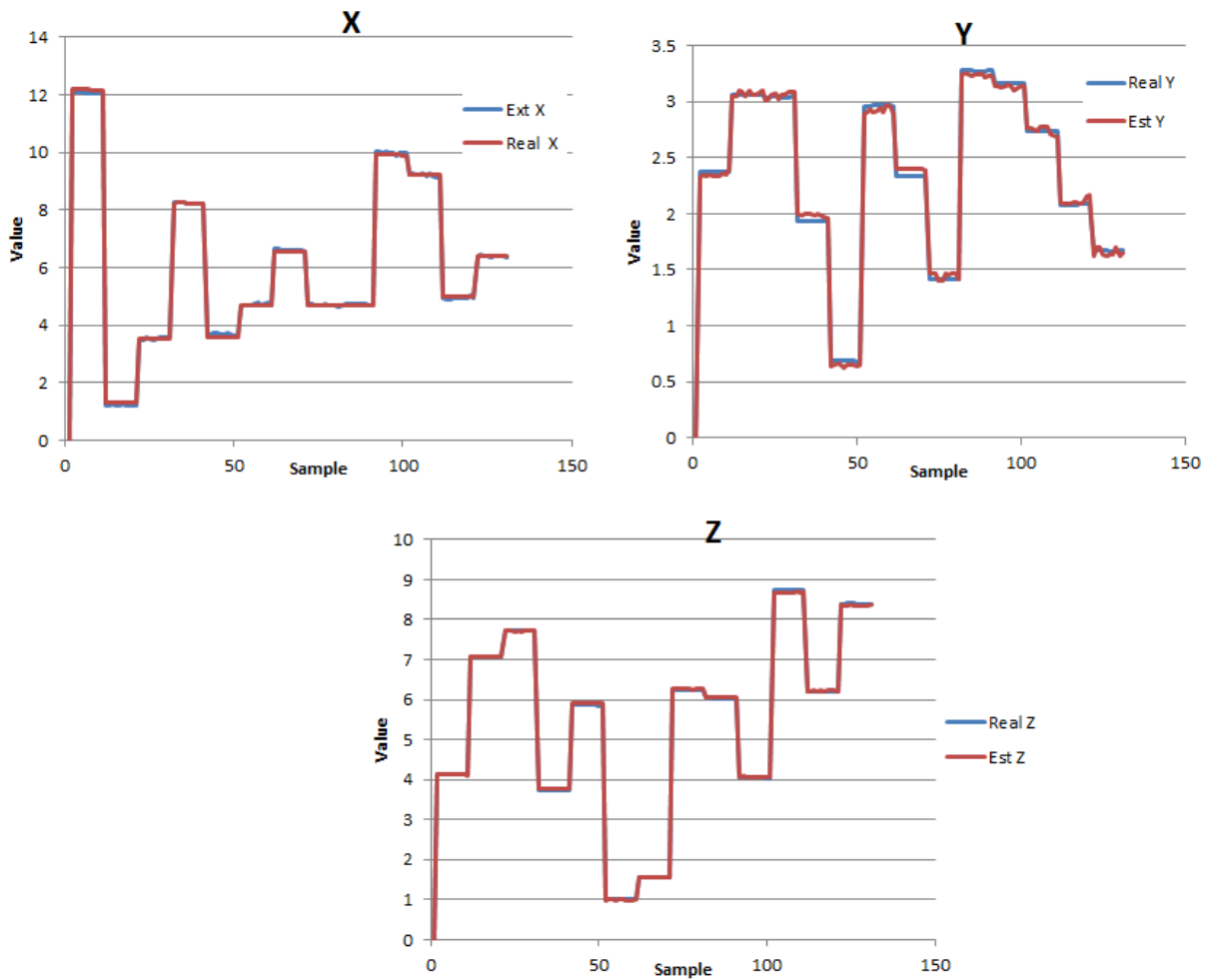


Figure 37: Photodiode calibration - without white LED

If we include the white LED in the calibration process, we obtain the result shown in Figure 38.

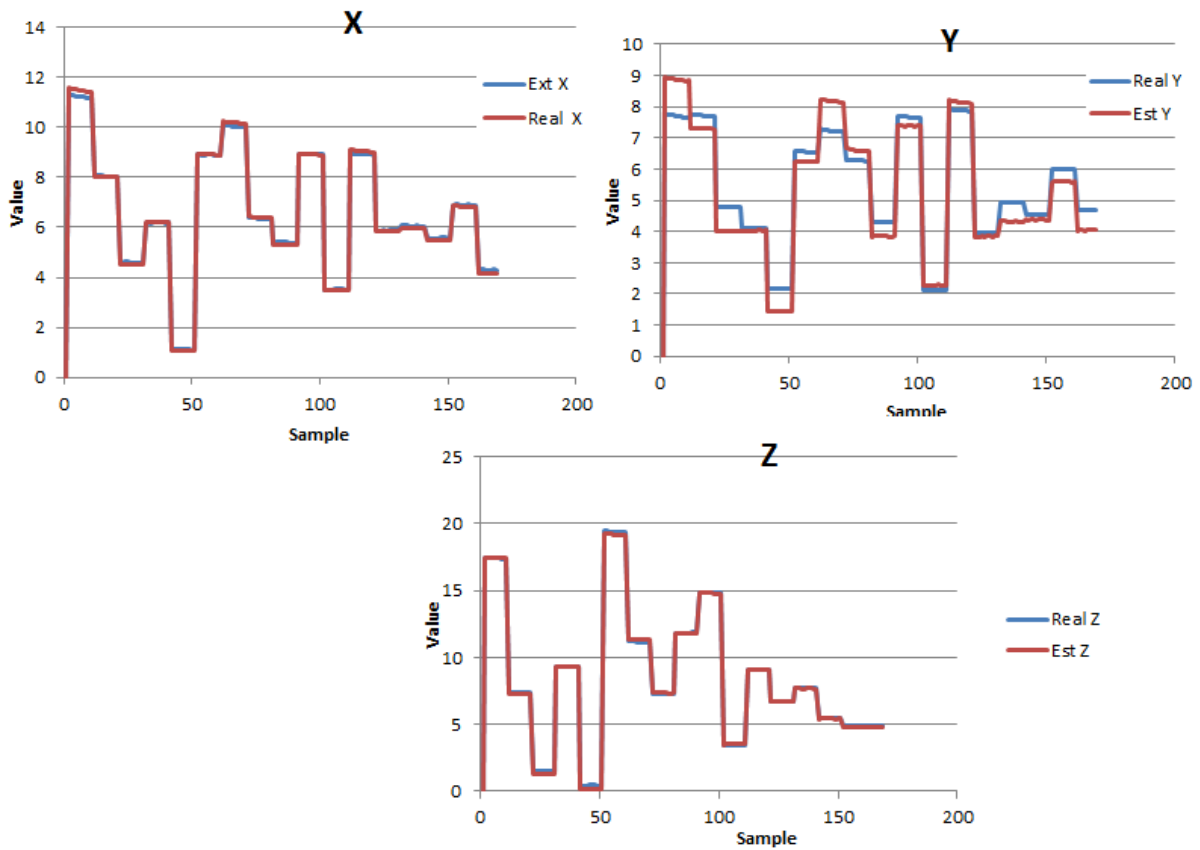


Figure 38: Photodiode calibration - with white LED

The average errors obtained from both experiments are summarized in Table 3.

Table 3: Calibration errors

		Error %		
	X	Y	Z	
No white	0.888348	1.549034	0.447014	
White	1.02701	8.473944	0.921374	

We observe that the Y variable is affected the most when we include the white LED in our experiment. Remembering that the Y variable is related to the response to green, the fact that the photodetector has a green filter that differs the most from the color matching functions explains why the inclusion of the white LED, which has a wider spectrum distribution, deteriorates this component more than the others.

In the other hand, from the CIE chromaticity diagram we see that the green regions are larger than the others. In fact, our perception to changes in chromaticity coordinates within the green region is less accurate than it is for the other regions.

6.5: Closed loop performance

After assuring that the system is able to identify the color of light being detected in the proper coordinates, we need to analyze the capability the system has to achieve the operation state set by the user.

The PI controller was chosen because of its capability of matching a constant reference with null error. As we discussed earlier, the time constants of the LEDs are negligible, much lower than those associated to the 5 KHz PWM signals we were using to drive them. The photodiodes have a rise time of 0.1 microseconds. Therefore, the dominant time constant in open loop is that of the filter, which is 0.1 milliseconds.

To find the parameters of the PI controller, we used the method Ziegler–Nichols method. It consists of first having a proportional controller inserted in the loop, whose value will be increased until the system starts to oscillate. The value of the proportional gain at this point is called K_u , and the period of the oscillation observed is called P_u . With these values in hand, we find K_p and T_i by:

$$K_p = \frac{K_u}{2.2} \quad T_i = \frac{P_u}{1.2}$$

After performing this experiment, we obtained the results in Figure 39. The values found were:

$$K_u = 1.9 \quad P_u = 0.122 \quad K_p = 0.86 \quad T_i = 0.102$$

Applying these values to the PI MIMO controller, we obtained the response characterized in Figure 40, with a rising time of about 0.3 seconds and null error (average of steady state value compared to the reference, disregarding noise). We then applied a considerable disturbance, activating the white LED with 0.5 duty cycle. In Figure 41 we see that the system rejects the step disturbance in about 0.8 seconds.

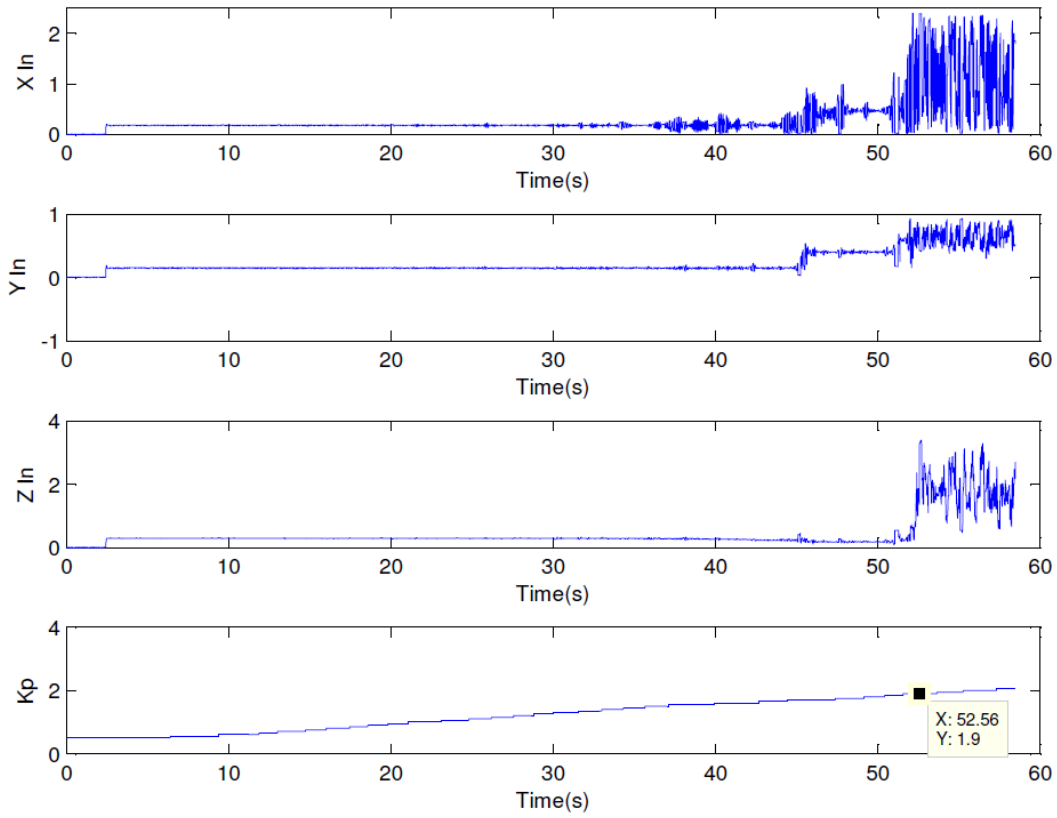


Figure 39: Finding the Ziegler-Nichols parameters k_u and P_u

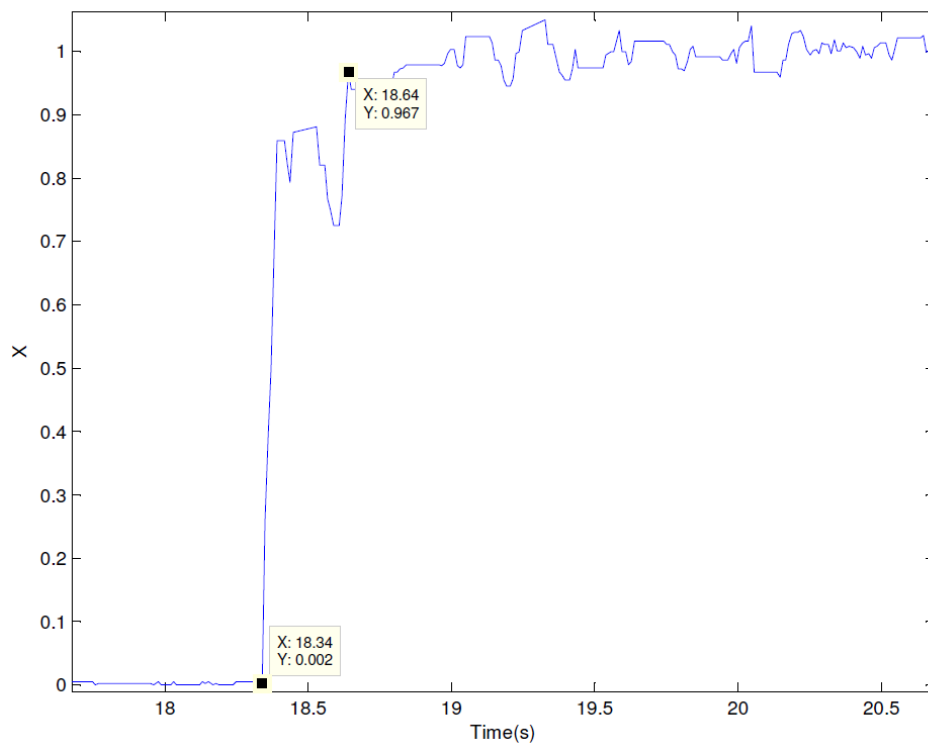


Figure 40: Step response - Closed loop

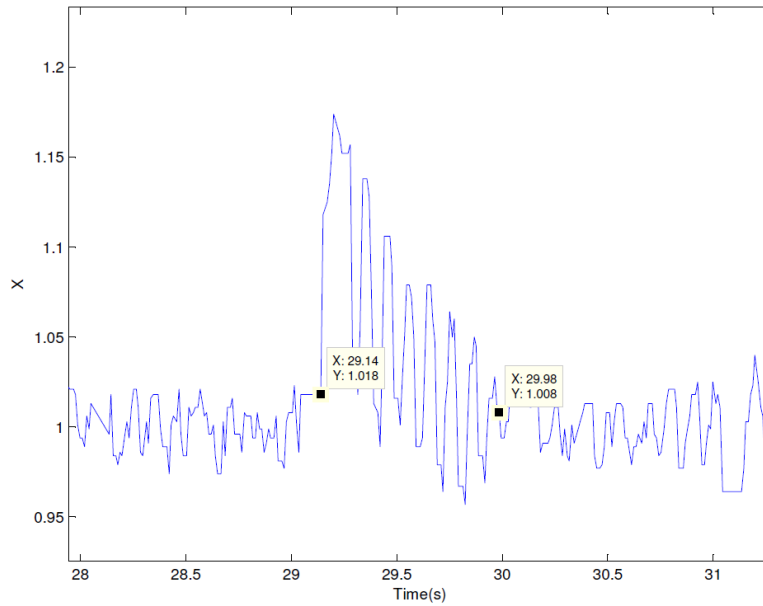


Figure 41: Disturbance rejection

As a rule of thumb, we set the tracking time T_t of the anti-windup term to be half of T_i . In order to compare the performance with and without the anti-windup calculation, we first set the output to a value outside the range of the LED and after an amount of time set it back within the range, to check how fast the system can respond. The results with and without anti-windup action are in *Figure 42*.

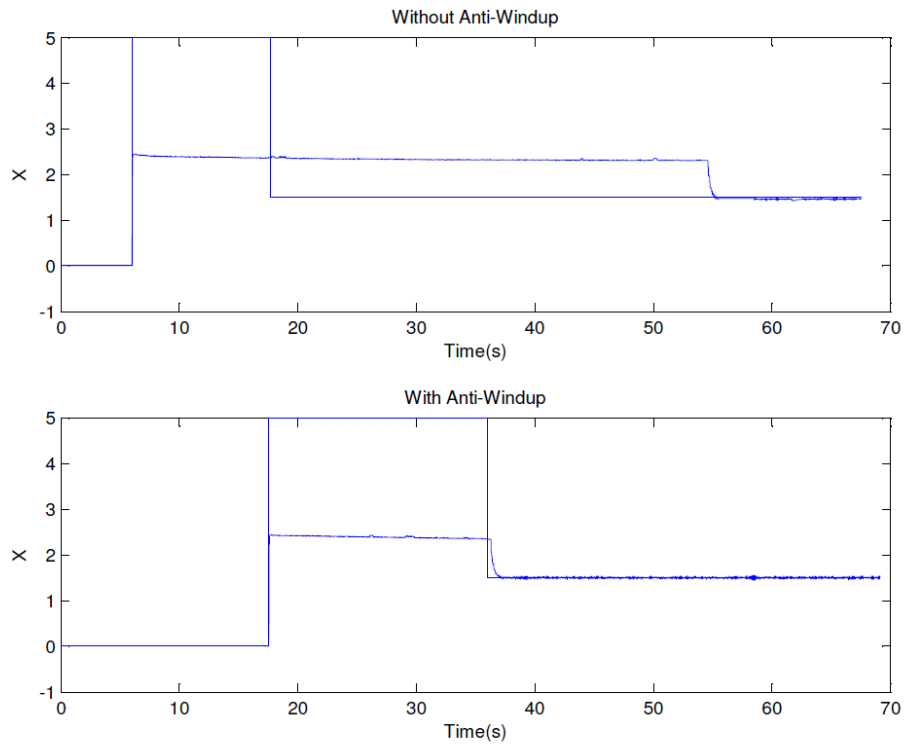


Figure 42: Comparison of system with and without anti-windup action

In the first case, after about 11 seconds with the system being saturated, the system takes additional 40 seconds to be able to respond to a new reference within the actuator range. In the second case, this time comes down to about 1 second, even when the time while the actuator was saturated was almost the double.

6.6: Costs

One of the objectives of his project was to obtain a solution involving low-cost technology. It is not our goal to match any pricing restriction at this point, but show that is possible to be achieved in a second moment. To provide a notion on the magnitude of prices involved, Table 4 shows the prices of the main components of the project.

Table 4: Components price

Component	Unity Price (US\$)	Source
Arduino Leonardo	\$21.50	http://microcontrollershop.com/product_info.php?products_id=4931
Cree® XLamp® MC-E Color LED	\$14.30	http://www.mouser.com/search/refine.aspx?Ntk=P_MarCom&Ntt=140602409
S9702 RGB Photodetector by Hamamatsu	\$12.95	http://www.datasheetarchive.com/buy/S9702.html
Other electronic components - estimated	\$5.00	
TOTAL	\$53.75	

In addition, a central computer and the I/O board was used. However, they may be replaced by the Arduino board in a potential future product.

7. Conclusion and perspectives

At the end of the project, we were able to demonstrate that the closed loop color control may be accomplished with the technologies we proposed.

- The PWM driving signal showed to be a very useful strategy to operate de LEDs in a linear way.
- The photodetectors we chose demonstrated to be capable of determining the color coordinates with an error that is within the range of non-perception by the standard observer.
- The PI control, with decoupling and back-calculation anti-windup strategy showed to be able to drive the LEDs to achieve any color of light within the achievable gamut.
- The system is capable of adapting itself in order to reject external disturbance, such as sun light, within the range of operation of the LEDs.
- The final estimated price of \$ 53.75 is considered to be low for a proof of concept, showing the potential of this solution.

In order to make this solution suitable to wider applications, the developments that are still to be done include:

- Embedding the central software to the Arduino board, which will replace the computer and the I/O board and carry out the color conversion, controller emulation and interface with the system. The calibration would still need to be done with a PC, but this can be done off-line, using a different system.
- Encapsulate the system, in order to make a closed final product.
- Demonstrate the capacity of the system to emulate any give chromaticity cycle, such as the natural sun light, based on color temperature reference coordinates.

Bibliography

1. **Bowman, David M, et al.** Fire in the Earth System. *Science*. 324, 2009, pp. 481-484.
2. **U.S. Department of Energy.** *2011 Buildings Energy Data Book*. s.l. : D&R International, Ltd., 2011.
3. **Lefèvre, Nicolas, de T'Serclaes, Philippine e Waide, Paul .** *Barriers To Technology Diffusion: The Case Of Compact Fluorescent Lamps*. INTERNATIONAL ENERGY AGENCY. 2006.
4. **Bullough, J D e Zhu, Y.** *Performance Objectives for Light Sources Used in Emergency Notification Appliances*. s.l. : Lighting Research Center, Rensselaer Polytechnic Institute, 2012.
5. **Nicola, Daniela.** *The Quest For Perfect Light*. s.l. : London South Bank University, 2010.
6. **Schubert, Fred E e Kim, Jong Kyu.** Solid-State Light Sources Getting Smart. *Science*. May, 2005, Vol. 308, pp. 1274-1278.
7. **Halper, Mark.** Does Siemens have world's most efficient LED? *Smart Planet*. [Online] 19 de April de 2012. <http://www.smartplanet.com/blog/intelligent-energy/does-siemens-have-worlds-most-efficient-led/15081>.
8. **U.S. Department of Energy.** *LED Frequently Asked Questions*. 2011.
9. **Curran, John W.** *Unraveling the Mysteries of Solid-State Lighting*. s.l. : LED Transformations, 2010.
10. **Karlicek, Robert.** *Smart Lighting: A Second Wave in Solid State Lighting?* s.l. : Rensselaer Polytechnic Institute, 2010.
11. **Sharma, Vijay Kumar.** Adaptive Significance of Circadian Clocks. *Chronobiology International*. November de 2003, Vol. 20, 6, pp. 901–919.
12. **Lockley, S W.** Circadian Rhythms: Influence of Light in Humans. [A. do livro] Larry R Squire. *Encyclopedia of Neuroscience*. s.l. : Elsevier, 2009, pp. 971-988.
13. **Philips Lumec.** The Effects of Artificial Light on Human. *Lumec.com*. [Online] Philips, October de 2010.

<http://www.lumec.com/newsletter/focal-point/10-2010/effects-artificial-light-humain.html>.

14. **Edgar, Rachel S., Green, W. Edward e et, al.** Peroxiredoxins are conserved markers of circadian rhythms. *Nature*. 485, May de 2012, pp. 459–464.

15. **Bedrosian, T A, Wei, Z M e Nelson, R J.** Chronic dim light at night provokes reversible depression-like phenotype: possible role for TNF. *Molecular Psychiatry*. July, 2012.

16. **Pauley, Stephen M.** Lighting for the Human Circadian Clock. Recent Research Indicates That Lighting Has Become a Public Health Issue. *Dark Sky Society*. [Online] March de 2004. <http://www.darksksociety.org/handouts/pauley.pdf>.

17. **Rea, Mark S.** Light - Much More Than Vision. *Lighting Research Center*. [Online] 2002. <http://www.lrc.rpi.edu/programs/lightHealth/pdf/moreThanVision.pdf>.

18. **Lewy, Alfred J., et al.** Bright artificial light treatment of a manic-depressive patient with seasonal mood cycle. *Am J Psychiatry*. 139, 1982, 11, pp. 1496-1498.

19. **Jack, L. e Wright, H.** The effect of evening bright light in delaying the circadian rhythms and lengthening the sleep of early morning awakening insomniacs. *Sleep*. 16, 1993, 5, pp. 436-443.

20. **Van Someren, Eus J W, et al.** Indirect bright light improves circadian rest-activity rhythm disturbances in demented patients. *Biol Psychiatry*. 41, 1997, pp. 955-963.

21. **Boyce, P, et al.** Lighting the graveyard shift: The influence of a daylight-simulating skylight on the task performance and mood of nightshift workers. *Lighting Research and Technology*. 9, 1997, 29, pp. 105-134.

22. **Figueiro, Mariana G, et al.** The effects of bright light on day and night shift nurses' performance and well-being in the NICU. *Neonatal Intensive Care*. 1, 2001, 14, pp. 29-32.

23. **Miller, C L, et al.** The effects of cycled versus noncycled lighting on growth and development in preterm infants. *Infant Behavior and Development*. 1995, Vol. 18, 1.

24. **Brandon, DH, Holditch-Davis, D e Belyea, M.** Preterm infants born at less than 31 weeks' gestation have improved growth in cycled light compared with continuous near darkness. *The Journal of Pediatrics*. 2002, Vol. 140, 2, pp. 192-199.
25. **Berson, DM, Dunn, FA e M, Takao.** Phototransduction by retinal ganglion cells that set the circadian clock. *Science*. 2002, Vol. 295, 5557, pp. 1070-1073.
26. **Hattar, S, et al.** elanopsincontaining retinal ganglion cells: architecture, projections, and intrinsic photosensitivity. *Science*. 2002, Vol. 295, 5557, pp. 1065-1070.
27. **Lewy, AJ, et al.** Light suppresses melatonin secretion in humans. *Science*. 1980, Vol. 210, 4475, pp. 1267-1269.
28. **Dauchy, RT, et al.** Dim light during darkness stimulates tumor progression by enhancing tumor fatty acid uptake and metabolism. *Cancer Letters*. 1999, Vol. 144, 2, pp. 131–136.
29. **Blask, D, et al.** Melatonin inhibition of cancer growth in vivo involves suppression of tumor fatty acid metabolism via melatonin receptor-mediated signal transduction events. *Cancer Research*. 1999, Vol. 59, 18, pp. 4693-4701.
30. **Badia, P, et al.** Bright light effects on body temperature, alertness, EEG and Behavior. *Physiology & Behavior*. 1991, Vol. 50, 3, pp. 583-588.
31. **Edelstein, Eve A, et al.** The Effects of Coulour and Light on Health. *World Health Design*. April, 2008.
32. **Grunert, Fred e Mahler, Winfried.** *What are the price advantages of light color regulation via feedback control?* Jena, Germany : Mazet, 2012.
33. **X-rite.** *The Color Guide and Glossary*. Grandville, MI : s.n., 2004.
34. **Grum, Franc C, Becherer, Richard e Bartleson, James .** *Optical radiation measurements*. s.l. : Academic Press, 1980.
35. **Barett, JT.** How to Drive an LED With Pwm. *E-How*. [Online] http://www.ehow.com/how_6186772_drive-led-pwm.html#ixzz2KvLjSPqi.
36. **Baker, Simon.** Pulse Width Modulation. *TFT Central*. [Online] February de 2012. http://www.tftcentral.co.uk/articles/pulse_width_modulation.htm.

37. **McNaught, A. D. e Wilkinson, A.** Compendium of Chemical Terminology. [A. do livro] IUPAC. *Gold Book*. Oxford : Blackwell Scientific Publications, 1997.
38. **Mynbaev, Djafar K. e Scheiner, Lowell L.** Photodiodes. [A. do livro] Djafar K. Mynbaev e Lowell L. Scheiner. *Fiber-Optic Communications Technology*. s.l. : Prentice Hall, 2006.
39. **Kang, Henry R.** *Computational Color Technology*. Bellingham, Washington USA : SPIE—The International Society for Optical Engineering, 2006. ISBN: 0-8194-6119-9.
40. **Bouman, C. A.** *Digital Image Processing*. 2012.
41. **Visioli, Antonio.** *Practical PID Control*. Brescia, Italy : Springer, 2006. ISBN-10: 1846285852.
42. **Åström, Karl Johan.** *Control System Design*. 2002.
43. **Markaroglu, Hayk, et al.** *Tracking Time Adjustment in Back Calculation Anti-Windup Scheme*. Istanbul, Turkey : Istanbul Technical University, 2006.
44. **Energy Information Administration.** *2003 Commercial Buildings Energy Consumption Survey*. 2003.